

A New Model for Cross-polarization Scattering from Perfect Conducting Random
Rough Surfaces in Backscattering Direction

by

Jiahao Cao

A Thesis Presented in Partial Fulfillment
of the Requirements for the Degree
Master of Science

Approved November 2017 by the
Graduate Supervisory Committee:

George Pan, Chair
Constantine A. Balanis
Douglas Cochran

ARIZONA STATE UNIVERSITY

December 2017

ABSTRACT

Scattering from random rough surface has been of interest for decades. Several methods were proposed to solve this problem, and Kirchhoff approximation (KA) and small perturbation method (SMP) are among the most popular. Both methods provide accurate results on first order scattering, and the range of validity is limited and cross-polarization scattering coefficient is zero for these two methods unless these two methods are carried out for higher orders. Furthermore, it is complicated for higher order formulation and multiple scattering and shadowing are neglected in these classic methods.

Extension of these two methods has been made in order to fix these problems. However, it is usually complicated and problem specific. While small slope approximation is one of the most widely used methods to bridge KA and SMP, it is not easy to implement in a general form. Two scale model can be employed to solve scattering problems for a tilted perturbation plane, the range of validity is limited.

A new model is proposed in this thesis to deal with cross-polarization scattering phenomenon on perfect electric conducting random surfaces. Integral equation is adopted in this model. While integral equation method is often combined with numerical method to solve the scattering coefficient, the proposed model solves the integral equation iteratively by analytic approximation. We utilize some approximations on the randomness of the surface, and obtain an explicit expression. It is shown that this expression achieves agreement with SMP method in second order.

ACKNOWLEDGMENTS

I would like to express my sincere gratitude to my advisor Dr. George Pan, for his valuable guidance and patience during the past two years. I am lucky to have the opportunity to continue to work with him for my PhD degree. He is very patient and is always there to help me. Also, he is knowledgeable and his way of thinking influences me a lot. I will benefit from his rigorous attitude and diligence on study for my life.

Besides my advisor, I would like to express my gratitude to the rest of my thesis committee for their presence and valuable comments. I would like to thank Dr. Constantine Balanis for teaching me antennas and electromagnetic. He taught me the skills and fundamentals on the area of electromagnetic, and he is always passionate on the course. Also, I want to thank Dr Douglas Cochran for his guidance on stochastic processes.

Furthermore, my sincere thanks go to my lab mates, Mr. Sai Zhou, Mr. Chin-Chieh Hsu and Mr. Kaiyue Zhang. Their kind help on both study and life is appreciated.

Finally, I would like to show my deepest appreciation to my friends and my family for their continuous support and encouragement.

TABLE OF CONTENTS

	Page
LIST OF TABLES	v
LIST OF FIGURES	vi
CHAPTER	
1 INTRODUCTION	1
1.1 Scattering from Random Rough Surface	1
1.2 Basic Concept	2
1.2.1 Random Roughness	3
1.2.2 Scattering Coefficient	4
2 CLASSIC THEORETICAL STUDIES ON RANDOM ROUGH SCAT- TERING	6
2.1 Kirchhoff Approximation	6
2.1.1 Formulation	7
2.1.2 Stationary-Phase Approximation	11
2.1.3 A Scalar Approximation	14
2.2 Small Perturbation Method	17
2.2.1 Formulation	17
2.3 Range of Validity for Kirchhoff Approximation and Small Pertur- bation Method	24
3 MODELING	26
3.1 Integral Equation	26
3.1.1 Electric Field Integral Equation	27
3.1.2 Magnetic Field Integral Equation	28
3.2 Surface Current	31
3.3 Far Field Backscattering Modeling	36

CHAPTER	Page
3.4 Scattered Power in Statistical Sense	38
4 NUMERICAL EVALUATION, RESULTS, AND FUTURE WORK	43
4.1 Numerical Method to Evaluate the Integral	43
4.2 Results and Comparison with Classic Model	47
4.3 Conclusion and Future Work	50
REFERENCES	52

LIST OF TABLES

Table	Page
2.1 Summary on Validity Conditions	24

LIST OF FIGURES

Figure	Page
2.1 Geometry of Kirchhoff method. $\hat{p} = \hat{v}$ in this case, which means the incident wave is vertically polarized	10
2.2 Geometry of Scattering Wave in Small Perturbation Method	18
2.3 Geometry of Scattered Wave in Spherical Coordinate	21
3.1 Evaluation of Limiting Value of the Integral When \vec{r}'' Approaches the Boundary	30
3.2 Geometry of the Surface Scattering Problem	33
3.3 Integral Contour for Inverse Fourier Transform	35
3.4 Geometry of the Reflected E Field	37
4.1 Sommerfeld Integration Path in Complex q Plane	45
4.2 A Robust Way of Defining an Integration Path	46
4.3 The Scattering Coefficient for $k\sigma = 0.2$ and $kl = 2.0$	47
4.4 The Scattering Coefficient for $k\sigma = 0.2$ and $kl = 2.4$	48
4.5 The Scattering Coefficient for $k\sigma = 0.1$ and $kl = 2.0$	49
4.6 The Scattering Coefficient for $k\sigma = 1.26$ and $kl = 3.77$	50

Chapter 1

INTRODUCTION

1.1 Scattering from Random Rough Surface

Wave scattering from random rough surface has been studied for decades and the interest remains strong due to the significance of the applications in diverse areas, such as imaging, communications, and remote sensing [27]. In particular, remote sensing in microwave range is among the most popular methods in remote sensing applications. Microwaves are suitable for different kinds of weathers, media and landscapes. In addition, compared to acoustic remote sensing, microwaves can travel faster and contain more information because of the existence of polarization. Electromagnetic waves can propagate through different media with very low loss while optical waves have more attenuation. It is easy to find an explicit solution for reflection and transmission from a planar boundary, however, scattering from rough surfaces is of practical benefit since most natural surfaces are not ideally planar. For instance, in remote sensing applications, both land surfaces and sea surfaces are irregular and knowledge of random rough scattering is helpful in these cases [14].

There are several methods to solve scattering problems. Empirical methods are the most straightforward, however, experimental conditions restrict the application of these methods. In remote sensing applications, it is impractical to measure all the parameters. Alternative way to deal with scattering is theoretical methods. Theoretical models consist of two different kind of models, numerical model and analytical model[10]. For numerical models, Monte-Carlo simulation should be employed which leads to high complexity of computation[12]. Method of moments combined with

Rao-Wilton-Glisson (RWG) basis functions is a popular method to deal with scattering issue numerically. Some progress are made to reduce the complexity of the numerical model with the introduction of wavelets [16][30]. Nevertheless, numerical models require computational space and are time consuming. Analytical models provide a method to deal with scattering more efficiently. While Maxwell equation and boundary conditions governing the scattering problem can not be solved analytically in closed-form under irregular boundary conditions, it is convenient to make some assumptions and approximations. Most famous early developed approaches are Kirchhoff approximation and small perturbation method, which are still widely used[23]. However, they all have limited domain of validity, and people are working to build a bridge between these two classic methods[11][7]. Small slope approximation(SSA)is among the most widely used methods [26]. SSA is still of interest and extension has been made to solve different kinds of scattering problems [13] [15]. And local curvature approximation is one of the successful extensions of SSA [6][5].

Backscattering is a special case in scattering problem and backscattering is of practical importance because of the wide applications such as communication, remote sensing and medical applications. While both numerical and analytical methods have been developed to solve co-polarization problems, cross-polarization has not been studied as much as co-polarization. Nevertheless, cross-polarization is as significant as co-polarization. In this thesis, cross-polarization is studied and an analytical model is established.

1.2 Basic Concept

Before getting started, basic concept should be established. In this thesis, only scatterings occurring between two different semi-infinite materials are under consid-

eration. When electromagnetic wave propagates towards the surface boundary, if the boundary is planar, reflection and refraction takes place. However, when the surface is rough, the wave can be reflected to many directions, and in practice, backscattering is of most significance in remote sensing application. In addition, if the medium is not homogeneous, some of the transmitted wave may be scattered back to the first medium, which is called volume scattering. Fortunately, in remote sensing applications, it is okay to assume the sea to be homogeneous since the electromagnetic property does not change a lot in different depth.

1.2.1 *Random Roughness*

In practice, sea surface is not deterministic, it has perturbations. The surface roughness can be modeled as stochastic process such that scattered power can be obtained in statistical sense, if we have the distribution of height probability and correlation length. In general, two parameters are commonly used in analytical methods. The first one is the standard deviation of the surface height, or root-mean-square(rms) height, noted by σ , which represents height variation. The other one is surface correlation length, noted by l , which stands for variation on horizontal directions. Typically, σ and l are expressed in terms of wavelength. And these two parameters form the concept of surface roughness. In particular, rms slope is one of the most popular parameters used to describe the surface roughness. When autocorrelation function of the surface is Gaussian, the rms slope can be expressed as

$$m = \sqrt{2} \frac{\sigma}{l} \tag{1.1}$$

1.2.2 Scattering Coefficient

Radar cross section (RCS) is a far-field parameter characterizing the scattering property of a radar target[2]. It is defined as the ratio of power of the reflected signal from a target to the reflected signal from a perfectly smooth sphere of cross sectional area of unit area. In general,

$$\frac{P_r}{P_t} = \frac{1}{4\pi r^2} G_t \sigma \frac{1}{4\pi r^2} \quad (1.2)$$

where P_t is the input power of the transmitter, G_t is the gain of the transmitter, and r is the distance between the target and antenna, and σ is the radar cross section.

However, this definition of RCS can not be applied to infinite surface, such as sea surface in remote sensing. In addition, polarization is not included in this RCS definition. In order to generalize it to extended surface, the concept of scattering coefficient is introduced. Scattering coefficient is defined as average RCS per unit area, and it is often noted by σ^0 . Scattering coefficient is a function of several parameters, such as system parameters(parameters dependent on the antenna part, i.e., frequency, polarization, incident angle and angle of observation) and target parameters(parameters dependent on the surface, i.e. surface roughness and permittivity). In order to show the dependence on polarization more explicitly, we attach subscripts on σ^0 and the received power. In the following equation(1.3), p and q denotes receiver polarization and transmitter polarization, respectively.

$$P_{qp} = \iint_{A_0} \frac{P_t G_t}{(4\pi)^2 r^4} \sigma_{qp}^0 ds \quad (1.3)$$

where A_0 is the illuminated area. σ^0 is assumed to be independent of surface coordinates throughout this thesis, thus, the integral in (1.3) can be replaced by simple multiplication.

$$P_{qp} = \frac{P_t A_0 G_t}{(4\pi)^2 r^4} \sigma_{qp}^0 \quad (1.4)$$

Taking circular attenuation into consideration, the power at receiver can be expressed as $P_{pqr} = P_{qp}/4\pi r^2$. Thus, rearrange (1.3), one can get

$$P_{qpr} = \frac{P_t A_0 G_t}{4\pi r^2} \sigma_{qp}^0 \quad (1.5)$$

In theoretical studies of random rough scattering, the average of σ_{qp}^0 is of interest since it is available to carry out and this parameter represents the property of an extended target in remote sensing applications. Cross-polarization backscattering has not been discussed much[8].

Chapter 2

CLASSIC THEORETICAL STUDIES ON RANDOM ROUGH SCATTERING

Theoretical studies focus on the derivation of σ^0 for extended targets as in Kirchhoff approximation and small perturbation method. These two methods were developed in 1960s, while they are still widely used and provides accurate results. Extension of these two methods were made from then, and attempt to bridge these two methods has not ceased. In this chapter, classic formulation and application of these two methods are introduced.

2.1 Kirchhoff Approximation

Kirchhoff approximation(also referred to tangent plane approximation or physical optics approximation) is one of the most widely used tools to solve surface-scattering problems. This method has a range of validity, it applies to high frequency incident waves. High frequency means small wavelength, and it is equivalent to the statement that the correlation length of the surface is large relative to the incident wavelength. As a result, it is reasonable to assume that any point at the surface can be regarded as an infinitely extended tangent plane and the total field is the sum of field reflected at every single point. On other words, reflection is specular at any point locally. And this tangent plane approximation is the basic assumption of Kirchhoff method. This assumption is valid when every point on the surface has a large radius of curvature compared to the wavelength of incident wave, which is the same as the statements before.

Under tangent plane approximation, the total field of a single point on the surface is the superposition of incident field and reflected field. Thus, the total field equal

the sum of incident field and the reflected field by an infinite extended plane tangent to the point.

2.1.1 Formulation

A linear polarized plane wave is considered throughout this thesis. Although in practice, there does not exist a monochromatic wave, the incident wave emitted by radar has little dispersion such that single frequency approximation does not produce significant errors. Thus, monochromatic wave is considered to simplify the calculation. Note that a time harmonic factor $e^{j\omega t}$ is omitted in every field terms throughout this paper. According to the properties of Helmholtz equation, the field on a source-free upper half plan is uniquely determined by the boundary condition. With the help of vector second Green's theorem and dyadic Green's function, the electric field satisfying radiation boundary condition can be expressed in integral form. [3] [1]

$$\vec{E}(\vec{r}) = \vec{E}^i(\vec{r}) + \int_S [-j\omega\mu\mathbf{G}(\vec{r}, \vec{r}')\hat{n}' \times \vec{H}(\vec{r}') - \nabla \times \mathbf{G}(\vec{r}, \vec{r}')\hat{n}' \times \vec{E}(\vec{r}')] ds \quad (2.1)$$

where $\mathbf{G}(\vec{r}, \vec{r}')$ is dyadic Green's function which satisfies (2.2), and \hat{n} is the unit normal vector pointing to the upper half plane.

$$\nabla \times \nabla \times \mathbf{G}(\vec{r}, \vec{r}') - k_0^2\mathbf{G}(\vec{r}, \vec{r}') = -\mathbf{I}\delta_3(\vec{r} - \vec{r}') \quad (2.2)$$

where k_0 is the wavenumber, \vec{r} represents observation vector, \vec{r}' means source position, \mathbf{I} is the identity matrix and $\delta_3(\vec{r} - \vec{r}')$ stands for 3-D Dirac-delta function, and it is defined by (2.3).

$$\delta_3(\vec{r} - \vec{r}') = \delta(x - x')\delta(y - y')\delta(z - z') \quad (2.3)$$

After some calculation, the above equation can be rearranged as

$$\nabla \times \nabla \times \mathbf{G}(\vec{r}, \vec{r}') + k_0^2\mathbf{G}(\vec{r}, \vec{r}') = (\mathbf{I} + \nabla\nabla/k^2)\delta_3(\vec{r} - \vec{r}') \quad (2.4)$$

where $G(\vec{r}, \vec{r}')$ is the Green's function for 3-D scalar wave equation(2.5).

$$\nabla^2 G(\vec{r}, \vec{r}') + k_0^2 G(\vec{r}, \vec{r}') = -\delta_3(\vec{r} - \vec{r}') \quad (2.5)$$

Combine equation (2.4) and equation (2.5), it is indicated that dyadic Green's function can be replaced by scalar Green's function $G(\vec{r}, \vec{r}')$.

$$\mathbf{G}(\vec{r}, \vec{r}') = (\mathbf{I} + \nabla\nabla/k^2)G(\vec{r}, \vec{r}') \quad (2.6)$$

It is obvious that field of any point is the superposition of incident field and scattered field.

$$\vec{E}(\vec{r}) = \vec{E}^i(\vec{r}) + \vec{E}^s(\vec{r}) \quad (2.7)$$

Compare (2.1) and (2.7), the first part on right hand side of (2.1) is the contribution of incident wave, while the second part denotes the contribution of the scattered wave and as shown in the equation, this part is due to the existence of surface. Therefore, the scattered wave field can be written as

$$\vec{E}^s(\vec{r}) = \int_S [-j\omega\mu\mathbf{G}(\vec{r}, \vec{r}')\hat{n}' \times \vec{H}(\vec{r}') - \nabla \times \mathbf{G}(\vec{r}, \vec{r}')\hat{n}' \times \vec{E}(\vec{r}')]dS \quad (2.8)$$

Solve equation (2.5) in polar coordinates, scalar Green's function can be expressed as

$$G(\vec{r}, \vec{r}') = -\frac{e^{-jk_0|\vec{r}-\vec{r}'|}}{4\pi|\vec{r}-\vec{r}'|} \quad (2.9)$$

When the observation is in far field region, in the denominator, $|\vec{r} - \vec{r}'| \simeq |\vec{r}| = r$, while in the numerator, $|\vec{r} - \vec{r}'|$ is in the phase, so the first two orders of the expansion is kept, namely, $|\vec{r} - \vec{r}'| \simeq r - \hat{r} \cdot \vec{r}'$ (\hat{r} means unit vector on \vec{r} direction). Based upon these two approximations, Stratton-Chu integral in terms of field components can be derived when we extend the integral domain S to infinity.[23]

$$\vec{E}^s = -C \times \hat{k}_s \times \int [\hat{n} \times \vec{E} - \eta\hat{k}_s \times (\hat{n} \times \vec{H})]e^{j\vec{k}_s \cdot \vec{r}}dS \quad (2.10)$$

where \hat{n} is the unit normal vector pointing outwards the surface, \vec{k}_s denotes the scattered direction, and C is a attenuation factor of circular wave. C and \hat{n} can be expressed by equation (2.11).

$$\begin{aligned}\hat{n} &= \frac{-\hat{x}Z_x - \hat{y}Z_y + \hat{z}}{\sqrt{1 + Z_x^2 + Z_y^2}} \\ C &= \frac{jk_0}{4\pi R} e^{-jk_0 R}\end{aligned}\tag{2.11}$$

where Z_x and Z_y are the surface derivatives with respect to x and y .

As indicated in equation (2.10), the scattered field can be implied as long as the tangential component of the field $\hat{n} \times \vec{E}$ and $\hat{n} \times \vec{H}$ are found. Most widely employed Kirchhoff approximation uses local frame of reference in terms of incident electrical polarization vector. And Fresnel reflection coefficient varies at different points as the angle of incidence changes. Assume the incident electric field to be

$$\vec{E}^i = \hat{p}E_0 e^{-j\vec{k}\cdot\vec{r}}\tag{2.12}$$

where E_0 is the amplitude of incident wave, \hat{p} is the direction of electric field which indicates the type of polarization.

Only linear polarization is considered in this thesis for ease of derivations. Furthermore, other kind of polarization can be reconstructed by two basic kinds of linear polarization of whom the vectors \hat{p} are orthogonal, namely, horizontal polarization and vertical polarization.(In some literature, they are also referred to perpendicular polarization and parallel polarization, respectively)

As shown in Figure 2.1, x, y and z forms a pair of global coordinates, while \hat{k}, \hat{h} and \hat{v} makes up local coordinates. In fact, the incident wave can be decomposed into a horizontal and a vertical component, by take the dot product with \hat{h} and \hat{v} . The tangential component $\hat{n} \times \vec{E}$ and $\hat{n} \times \vec{H}$ can be expressed as sum of the tangential vertically polarized field and tangential horizontally polarized field. And

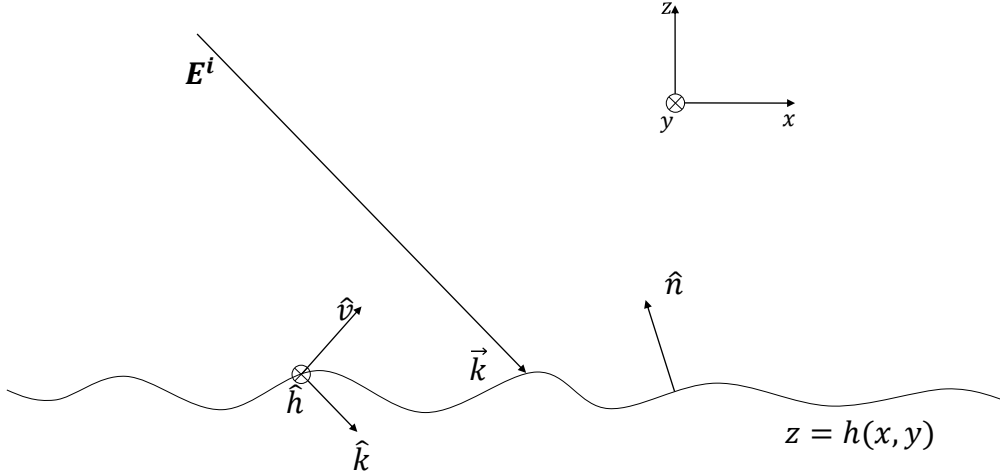


Figure 2.1: Geometry of Kirchhoff method. $\hat{p} = \hat{v}$ in this case, which means the incident wave is vertically polarized

scattered field is written in terms of incident field and Fresnel reflection coefficient.

The scattered field can be obtained after trivial calculation

$$\begin{aligned}\hat{n} \times \vec{E} &= [(1 + R_h)(\hat{p} \cdot \hat{h})(\hat{n} \times \hat{h}) - (1 - R_v)(\hat{n} \cdot \hat{k})(\hat{p} \cdot \hat{v})\hat{h}]E_0e^{-j\vec{k} \cdot \vec{r}} \\ \hat{n} \times \vec{H} &= -\frac{1}{\eta}[(1 - R_h)(\hat{n} \cdot \hat{k})(\hat{p} \cdot \hat{h})\hat{h} + (1 + R_hv)(\hat{p} \cdot \hat{v})(\hat{n} \times \hat{h})]E_0e^{-j\vec{k} \cdot \vec{r}}\end{aligned}\quad (2.13)$$

Substitute equation (2.13) into equation (2.10), the scattered field can be written as

$$\vec{E}^s = -C \times \hat{k}_s \times \int [\hat{n} \times \vec{E} - \eta \hat{k}_s \times (\hat{n} \times \vec{H})] e^{j(\vec{k}_s - \vec{k}) \cdot \vec{r}'} dS' \quad (2.14)$$

The physical meaning of the above equation is that the scattered wave can be seen as the superposition of the scattered waves over the illuminated area along with a phase factor $e^{-j\vec{k} \cdot \vec{r}'}$. However, analytical solution to equation (2.14) is still difficult to be obtained without further simplifying assumptions. There are two common assumptions called stationary-phase approximation (also referred to geometric optics approximation) and scalar approximation (physical optics approximation). The former approximation works for surfaces with large variations of heights compared to wavelength of incident wave, while the latter is applied to surfaces with small slopes and small or medium variations of heights.

2.1.2 Stationary-Phase Approximation

Stationary-phase approximation is based on an assumption that scattering only happens along directions for which there are specular points on the surface. This means local diffraction effects is ignored in this assumption. Phase Q is defined as

$$Q = (\vec{k}_s - \vec{k}) \cdot \vec{r}' \equiv q_x x' + q_y y' + q_z z' \quad (2.15)$$

Assume that the surface is a linear system, which means frequency remains the same in the scattered wave. That is to say, $|\vec{k}_s| = |\vec{k}|$, and denote this magnitude by k . It is convenient to expand \vec{k}_s and \vec{k} in spherical coordinates, and hence Q can be written in terms of spherical expansions.

$$\begin{aligned} \hat{k}_s &= \hat{x} \sin\theta_s \cos\phi_s + \hat{y} \sin\theta_s \sin\phi_s + \hat{z} \cos\theta_s \\ \hat{k} &= \hat{x} \sin\theta \cos\phi + \hat{y} \sin\theta \sin\phi - \hat{z} \cos\theta \end{aligned} \quad (2.16)$$

Thus q_x, q_y and q_z can be expressed as

$$\begin{aligned} q_x &= k[\sin\theta_s \cos\phi_s - \sin\theta \cos\phi] \\ q_y &= k[\sin\theta_s \sin\phi_s - \sin\theta \sin\phi] \\ q_z &= k[\cos\theta_s + \cos\theta] \end{aligned} \quad (2.17)$$

Q is stationary means that Q is a constant hence the partial derivatives of Q are 0.

$$\begin{aligned} \frac{\partial Q}{\partial x} &= 0 = q_x + q_z \frac{\partial z}{\partial x} \\ \frac{\partial Q}{\partial y} &= 0 = q_y + q_z \frac{\partial z}{\partial y} \end{aligned} \quad (2.18)$$

Rearrange the above equations, the partial derivatives of surface heights can be written in terms of the components of phase.

$$\begin{aligned} Z_x &= \frac{\partial z}{\partial x} = -\frac{q_x}{q_z} \\ Z_y &= \frac{\partial z}{\partial y} = -\frac{q_y}{q_z} \end{aligned} \quad (2.19)$$

According to equation (2.11), $\hat{n} \times \vec{E}$ and $\hat{n} \times \vec{H}$ is dependent on the surface derivatives. The introduction of stationary-phase approximation yields equation (2.19), which makes the tangential field components independent on the surface derivatives hence eliminates the dependence on integral variables. Therefore, the expression for \vec{E}^s can be simplified as shown in equation (2.20).

$$\vec{E}^s = -C \times \hat{k}_s \times [\hat{n} \times \vec{E} - \eta \hat{k}_s \times (\hat{n} \times \vec{H})] I_1 \quad (2.20)$$

where

$$I_1 = \int e^{j(\vec{k}_s - \vec{k}) \cdot \vec{r}'} dS' \quad (2.21)$$

The scattered field with polarization vector \hat{q} and incident polarization vector \hat{p} can be expressed by

$$E_{qp}^s = \hat{q} \cdot \vec{E}^s = C I_1 E_0 U_{qp} \quad (2.22)$$

where

$$U_{qp} = \frac{1}{E_0} \hat{q} \cdot \hat{k}_s \times [\hat{n} \times \vec{E} - \eta \hat{k}_s \times (\hat{n} \times \vec{H})] \quad (2.23)$$

Since power of electromagnetic wave is proportional to the square of the amplitude of electric field, an expression of scattering coefficient can be derived after we rearrange equation(1.5). [23]

$$\sigma_{qp} = \frac{4\pi r^2 |E_{qp}^s|^2}{A_0 |E^i|^2} \quad (2.24)$$

As shown in equation (2.24), the ensemble average of $|I_1|^2$ is required in order to calculate $|E_{qp}^s|^2$.

$$\langle |I_1|^2 \rangle = \langle I_1^* I_1 \rangle = \iint \langle e^{j(\vec{k}_s - \vec{k}) \cdot (\vec{r} - \vec{r}')} \rangle ds ds' \quad (2.25)$$

Gaussian and isotropic random process, which has a zero mean, standard deviation σ and correlation coefficient ρ , is assumed in this case. Furthermore, the standard

deviation is assumed to be large. Based upon these assumptions, equation (2.25) can be solved.

$$\langle |I_1|^2 \rangle = \frac{2\pi A_0 q^2}{q_z^4 \sigma^2 |\rho''(0)|} \exp\left[-\frac{q_x^2 + q_y^2}{2q_z^2 \sigma^2 |\rho''(0)|}\right] \quad (2.26)$$

where $\rho''(0)$ represents second derivative of correlation coefficient at the origin, and $\sigma^2 |\rho''(0)|$ is the same as mean-square slope of this random surface. [22]

Upon substituting equation (2.26) and equation (2.22) into equation (2.24), it follows

$$\sigma_{qp} = \frac{(kq^2 |U_{qp}|)^2}{2q_z^4 \sigma^2 |\rho''(0)|} \exp\left[-\frac{q_x^2 + q_y^2}{2q_z^2 \sigma^2 |\rho''(0)|}\right] \quad (2.27)$$

Throughout the derivation of equation (2.27), shadowing and multiple scattering are not taken into consideration. And backscattering is a case of special interest. Another pair of polarization vectors \hat{h}_s and \hat{v}_s , representing horizontal and vertical polarization of the scattered field, is introduced. It is easy to find the expressions of these two pairs of polarization vectors in terms of θ , ϕ , θ_s and ϕ_s . In backscattering case, $\theta_s = \theta$, $\phi_s = \pi$ and $\phi = 0$. Since backscattering occurs in the plane of incidence, which is orthogonal to horizontal polarization vector. Therefore, $\hat{h}_s \cdot \hat{k}$ and $\hat{h}_s \cdot \hat{k}_s$ vanishes. The expression of scattering coefficient in backscattering is shown below.

$$\sigma_{pp}\theta = \frac{|R_{pp}(0)|^2 e^{-(\tan^2 \theta / 2\sigma^2 |\rho''(0)|)}}{2\sigma^2 |\rho''(0)| \cos^4 \theta} \quad (2.28)$$

$$\sigma_{pq}\theta = 0 \quad (2.29)$$

where $R_{pp}(0)$ is the Fresnel reflection coefficient under normal incidence.

A disadvantage of this method is that, due to the neglect of multiple scattering, the cross-polarized scattering coefficient is 0. And also note that this model has limitations which states that the standard deviation of surface height must be large compared to incident wavelength. The physical interpretation is that when surface function has a large variance, the specular component becomes negligible as

the surface gets rougher hence the scattered field behaves stochastically. However, when variance becomes small, specular component(also referred to coherent scattering component) appears to influence the process, and when σ approaches zero, coherent scattering component dominates. When the variance is zero for the surface, it becomes a planar reflection, which is purely coherent. A different approximation for small variance is needed, which is called a scalar approximation.

2.1.3 A Scalar Approximation

A different approach is mentioned in this part, which is different from stationary-phase approximation. In stationary-phase approximation, Based upon the assumption that only specular reflection occurs on every tangential plane, the scattering is purely non-coherent, since the scattering only depends on the randomness of the surface. When surface becomes less rougher, the surface generates coherent scattering. Fortunately, as shown in equation (1.1), small standard deviation means small rms slope. Further approximation can be made since the surfaces are restricted to those with small slopes. Since the denominator of equation (2.11) contains second order of slope terms, these terms are ignored in this approximation, which implies

$$\hat{n} = -\hat{x}Z_x - \hat{y}Z_y + \hat{z} \quad (2.30)$$

This assumption leads to a decoupling of polarization in the vector scattering equations and hence reducing to scalar equations. Therefore, this assumption is called a scalar approximation. The power of scattered field can be obtained by taking Taylor expansion of Stratton-Chu integral in surface slope distribution. The expression of scattered field can be rewritten as

$$E_{qp}^s = CE_0 \int \bar{U}_{qp} e^{j(\vec{k}^s - \vec{k}) \cdot \vec{r}} ds \quad (2.31)$$

where \bar{U}_{qp} is defined in [23]. And since \bar{U}_{qp} is a function of unit normal vector and hence a function of surface slopes, one can expand it in Taylor series in terms of Z_x and Z_y and neglect all higher orders.

$$\bar{U}_{qp} = a_0 + a_1 Z_x + a_2 Z_y \quad (2.32)$$

where a_0 , a_1 and a_2 are related to polarization of incident and scattered wave.

$$I = \langle E_{qp}^s E_{qp}^{s*} \rangle = \iint \langle \bar{U}_{qp} \bar{U}_{qp}^* e^{j(\vec{k}_s - \vec{k}) \cdot (\vec{r} - \vec{r}')} \rangle ds ds' \quad (2.33)$$

$\bar{U}_{qp} \bar{U}_{qp}^*$ is required in order to obtain I and hence the scattering coefficient. Ignore all higher order items,

$$\bar{U}_{qp} \bar{U}_{qp}^* = a_0 a_0^* + a_0 a_1^* Z_x + a_0^* a_1 Z_x + a_0 a_2^* Z_y + a_0^* a_2 Z_y \quad (2.34)$$

Assume the illuminated area is $2L \times 2L$, and keep only the first term in equation (2.34), and substitute into equation (2.33), it follows

$$I_0 = |a_0|^2 \int_{-2L}^{2L} \int_{-2L}^{2L} (2L - |u|)(2L - |v|) e^{jq_x u + jq_y v} e^{-q_z^2 \sigma^2 (1-\rho)} du dv \quad (2.35)$$

In this assumption, standard deviation of surface height is small. Thus, Maclaurin expansion can be applied to term $e^{q_z^2 \sigma^2 \rho}$, yielding

$$I_0 = |a_0|^2 \sum_{n=0}^{\infty} \frac{(q_z^2 \sigma^2)^n}{n!} \int_{-2L}^{2L} \int_{-2L}^{2L} \rho^n (2L - |u|)(2L - |v|) e^{jq_x u + jq_y v} du dv \quad (2.36)$$

where $n = 0$ term stands for coherent scattering term. Further calculation implies that

$$\sigma_{qp}^0 = \pi k^2 |a_0|^2 \delta(q_x) \delta(q_y) e^{-q_z^2 \sigma^2} \quad (2.37)$$

The exponential term in equation (2.37) shows that the coherent scattering coefficient only matters when $q_z \sigma$ is small, which corresponds to the statement that the scattering is purely incoherent when standard deviation of the surface is large compared to the wavelength. Note that $q_z \sigma$ is proportional to σ/λ .

The rest of summation in equation (2.36) corresponds to incoherent component. Since illuminated area is large compared with correlation length, for $n \geq 1$, equation (2.36) can be approximated as

$$I_0 = |a_0|^2 A_0 \sum_{n=1}^{\infty} \frac{(q_z^2 \sigma^2)^n}{n!} \int_{-\infty}^{\infty} \int_{-\infty}^{\infty} \rho^n (2L - |u|)(2L - |v|) e^{jq_x u + jq_y v} dudv \quad (2.38)$$

Similarly as in stationary-phase approximation, stable isotropic Gaussian stochastic process is assumed in order to obtain an analytical expression of scattering coefficient.

$$\sigma_{qp}^0 \text{ inc} = (kl|a_0|)^2 e^{-q_z^2 \sigma^2} \sum_{n=1}^{\infty} \frac{(q_z^2 \sigma^2)^n}{n! n} \exp\left(-\frac{(q_x + q_y)^2 l^2}{4n}\right) \quad (2.39)$$

As standard deviation of the surface approaches zero, equation (2.39) tends to zero. It is to say, when surface become planar surface, only the specular reflection whose power intensity is governed by Fresnel reflection coefficient remains. An additional contribution to the total scattering coefficient is from the slope terms which is ignored in the above derivations. The derivations of this part is not important in this thesis, thus it is not included. It was derived in [23] in detail. Also, we are interested at the special case of backscattering. BY geometry, a_0 in backscattering can be expressed as a function of incident angle θ .

$$\begin{aligned} a_0 &= 2R_h \theta \cos\theta && \text{for } HH \text{ polarization} \\ a_0 &= -2R_v \theta \cos\theta && \text{for } VV \text{ polarization} \\ a_0 &= 0 && \text{for } HV \text{ and } VH \text{ polarizations} \end{aligned} \quad (2.40)$$

As shown in equation (2.40), in a scalar approximation the cross-polarization scattering coefficient is also zero. However, this scattering coefficient exists in practice. In Kirchhoff approximation, the average radius of curvature is required to be large compared to the incident wavelength.

2.2 Small Perturbation Method

For Kirchhoff approximation, the basic assumption must be satisfied thus high frequency is required. However, when this condition does not hold, alternative method should be proposed. The small perturbation method is applied to a slightly rough surface.

2.2.1 Formulation

First of all, Fourier transform of the surface height function $z = h(x, y)$ is needed.

$$\begin{aligned} \tilde{Z}(u, v) &= \iint_{-\infty}^{\infty} z(x, y) e^{-jux-jvy} dx dy \\ z(x, y) &= \frac{1}{2\pi} \iint_{-\infty}^{\infty} \tilde{Z}(u, v) e^{jux+jvy} du dv \end{aligned} \tag{2.41}$$

A classical way to solve Helmholtz equation is separation of variables, however, it is hard to employ this method since the boundary condition is complicated. Fortunately, utilize Fourier transform and assume the wave propagates in the xz plane. Another assumption applied in the calculation is that only wave propagates to $+z$ direction is taken into consideration. Actually, there exists some waves traveling in $-z$ direction at surface points of larger height and larger slope, however, the wave traveling to $-z$ direction encounters second reflection and travels upwards after multiple scattering. Also, in far-field, only waves propagating upwards survive. There are different combinations of incident polarization and scattered polarization. A horizontal polarized wave (See Figure (2.2)) is utilized as the start point for this section. This is the same with Rayleigh Hypothesis stated in [26]. Figure (2.2) shows the geometry of this problem.

For horizontal polarized incident wave, the electric field amplitude on polarization direction should be the sum of incident wave, coherent reflected wave and incoherent

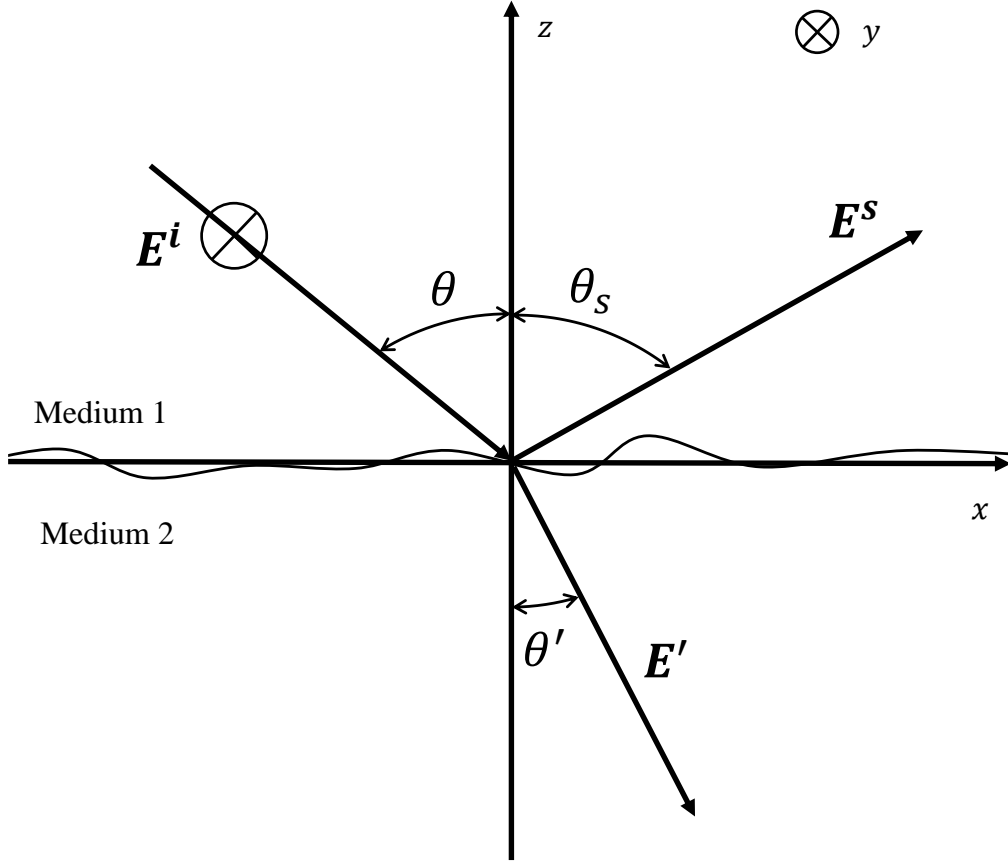


Figure 2.2: Geometry of Scattering Wave in Small Perturbation Method

reflection.

$$\begin{aligned}
 E_x &= \frac{1}{2\pi} \iint_{-\infty}^{\infty} U_x(k_x, k_y) \exp(jk_x x + jk_y y - jk_z z) dk_x dk_y \\
 E_y &= \frac{1}{2\pi} \iint_{-\infty}^{\infty} U_y(k_x, k_y) \exp(jk_x x + jk_y y - jk_z z) dk_x dk_y + \\
 &\quad E_0 e^{-jk_x \sin \theta} (e^{jk_z \cos \theta} + R_h e^{-jk_z \cos \theta}) \\
 E_z &= \frac{1}{2\pi} \iint_{-\infty}^{\infty} U_z(k_x, k_y) \exp(jk_x x + jk_y y - jk_z z) dk_x dk_y \\
 k_z^2 &= k^2 - k_x^2 - k_y^2
 \end{aligned} \tag{2.42}$$

where U_x , U_y and U_z are unknown amplitude in spatial frequency domain. Similarly,

the field amplitude in medium 2 can be written as

$$\begin{aligned}
E'_x &= \frac{1}{2\pi} \iint_{-\infty}^{\infty} D_x(k_x, k_y) \exp(jk_x x + jk_y y + jk'_z z) dk_x dk_y \\
E'_y &= \frac{1}{2\pi} \iint_{-\infty}^{\infty} D_y(k_x, k_y) \exp(jk_x x + jk_y y + jk'_z z) dk_x dk_y + E_0 T_h (e^{-jk' x \sin \theta} + e^{jk' z \cos \theta}) \\
E'_z &= \frac{1}{2\pi} \iint_{-\infty}^{\infty} D_z(k_x, k_y) \exp(jk_x x + jk_y y + jk'_z z) dk_x dk_y \\
k'_z &= k'^2 - k_x^2 - k_y^2
\end{aligned} \tag{2.43}$$

where k' is the wavenumber in medium 2, T_h is the Fresnel transmission coefficient for horizontal polarization and D_x, D_y and D_z are unknown field amplitude in medium 2 correspondingly. Actually, the above equation does not satisfy the conservation of energy, which is the same as in Rayleigh Hypothesis. In order to achieve conservation of energy, the coherent scattering and transmitted terms should be modified. However, in this thesis, for ease of calculation and simplicity, modifications of Fresnel coefficient is not taken in to consideration. [19]

The unknown amplitude is determined by divergence relations and boundary conditions which is affected by the geometry of the surface and the electromagnetic properties of two media. Equation (2.44) shows these relations.

$$\begin{aligned}
\hat{n} \times (\vec{E} - \vec{E}') &= 0 \\
\hat{n} \times (\vec{H} - \vec{H}') &= 0 \\
\nabla \cdot \vec{E} &= 0
\end{aligned} \tag{2.44}$$

where \hat{n} can be expressed in terms of surface slope as shown in equation (2.11).

Six scalar equations can be extracted from the above relations, which can be utilized to determine six unknowns, namely, U_x, U_y, U_z and D_x, D_y, D_z . In small perturbation method, $k_z z$ and $k'_z z$ is assumed to be small, as a result, it is reasonable to expand all exponential terms involving kz in Taylor series. Furthermore, the field

amplitudes can be expanded in a perturbation series as shown in equation (2.45)

$$\begin{aligned} U_x &= U_{x1} + U_{x2} + U_{x3} + \dots \\ D_x &= D_{x1} + D_{x2} + D_{x3} + \dots \end{aligned} \quad (2.45)$$

Substitute equation (2.45) into equation (2.42) and do Taylor expansion, then it follows

$$\begin{aligned} E_x &= \frac{1}{2\pi} \iint_{-\infty}^{\infty} (U_{x1} + U_{x2} + \dots)(1 - jk_z z - \dots) \exp(jk_x x + jk_y y) dk_x dk_y \\ E'_x &= \frac{1}{2\pi} \iint_{-\infty}^{\infty} (D_{x1} + D_{x2} + \dots)(1 + jk'_z z + \dots) \exp(jk_x x + jk_y y) dk_x dk_y \end{aligned} \quad (2.46)$$

Similarly, the y and z components can be expressed in terms of series. And substitute the expressions of electric field into the relations, six algebraic equations can be found for six unknown amplitudes.

$$\begin{aligned} U_{x1} &= D_{x1} \\ U_{y1} &= D_{y1} - jk' \cos(\theta') (1/\mu_r - 1) T_h \tilde{Z}(k_x + k \sin\theta, k_y) \\ k_x (U_{z1} - D_{z1}/\mu_r) + k_z U_{x1} + k'_z D_{x1}/\mu_r + \beta_1 &= 0 \\ k_x (U_{z1} - D_{z1}/\mu_r) + k_z U_{x1} + k'_z D_{x1}/\mu_r + \beta_2 &= 0 \\ k_z U_{z1} &= k_x U_{x1} + k_y U_{y1} \\ k'_z D_{z1} &= -(k_x D_{x1} + k_y D_{y1}) \end{aligned} \quad (2.47)$$

where \tilde{Z} is the Fourier transform of surface height function as shown in equation (2.41) β_1 and β_2 is expressed as follows.

$$\begin{aligned} \beta_1 &= jkk_y \sin\theta (1 - 1/\mu_r) T_h \tilde{Z}(k_x + k \sin\theta, k_y) \\ \beta_2 &= jT_h \left[\frac{k'^2 \cos^2(\theta')}{\mu_r} - k^2 \cos^2\theta - (k_x + k \sin\theta) k \sin\theta \left(1 - \frac{1}{\mu_r}\right) \right] \tilde{Z}(k_x + k \sin\theta, k_y) \end{aligned} \quad (2.48)$$

Equation (2.47) can be solved. Once the six amplitudes is obtained, the scattered field of different polarization can be found. Since the start point of the derivation is

horizontal polarized wave, E_{hh} and E_{vh} can be calculated in terms of these amplitudes. As shown in Figure (2.3), the field amplitude of co-polarized (E_{hh}) and cross-polarized (E_{vh}) can be expressed in terms of spherical coordinate.

$$\begin{aligned} E_{hh} &= \hat{h} \cdot \vec{E}^s = \hat{\phi}_s \cdot \vec{E}^s \\ E_{vh} &= \hat{v} \cdot \vec{E}^s = \hat{\theta}_s \cdot \vec{E}^s \end{aligned} \quad (2.49)$$

Unit coordinate vector can be expressed as

$$\begin{aligned} \hat{\theta}_s &= \hat{x} \cos \theta_s \cos(\phi_s) + \hat{y} \cos \theta_s \sin \phi_s - \hat{z} \sin \theta_s \\ \hat{\phi}_s &= -\hat{x} \sin \phi_s + \hat{y} \cos \phi_s \end{aligned} \quad (2.50)$$

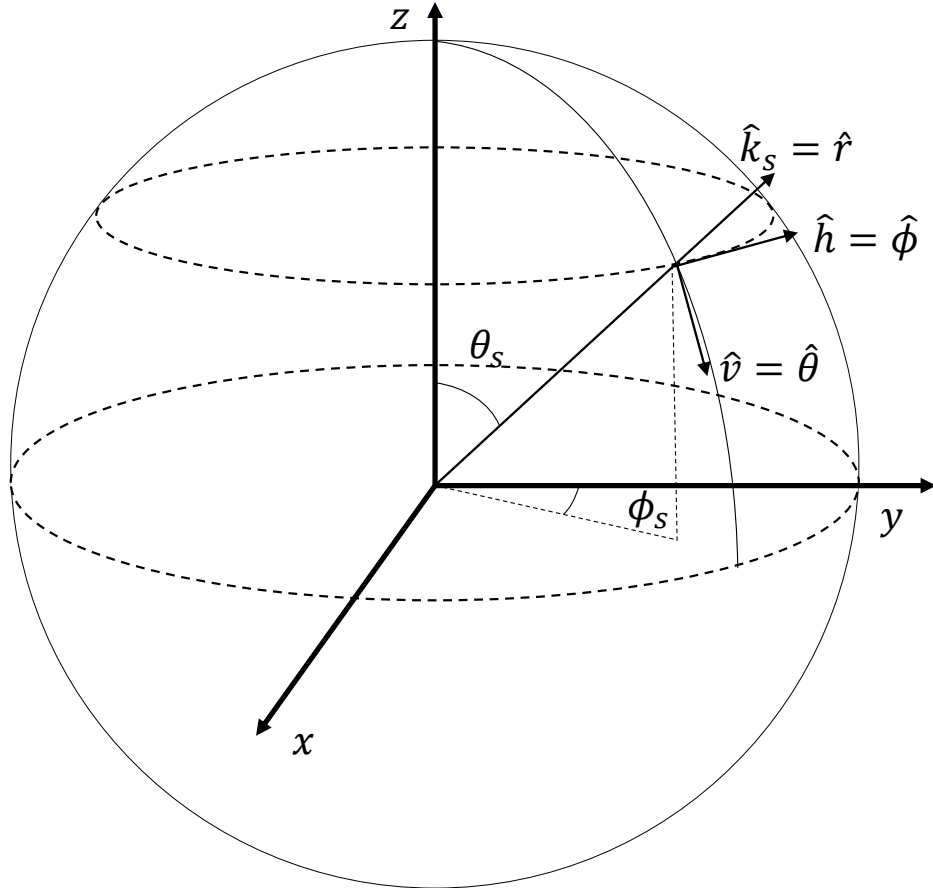


Figure 2.3: Geometry of Scattered Wave in Spherical Coordinate

where \hat{k}_s is the direction of wave propagation, and as shown in this figure, horizontal polarized vector is the same as $\hat{\phi}$ while vertical polarization vector is the same as $\hat{\theta}$. These geometrical relations allow us to express the scattered field in spherical coordinate.

Substitute equation (2.50) into equation (2.49), it follows

$$\begin{aligned} E_{hh} &= \frac{1}{2\pi} \iint [U_{y1} \cos\phi_s - U_{x1} \sin\phi_s] \exp(jk_x x + jk_y y - jk_z z) dk_x dk_y \\ E_{vh} &= \frac{1}{2\pi} \iint \frac{U_{x1} \cos\phi_s + U_{y1} \sin\phi_s}{\cos\theta_s} \exp(jk_x x + jk_y y - jk_z z) dk_x dk_y \end{aligned} \quad (2.51)$$

When scattered field is obtained, scattering coefficient can be found in terms of the ensemble average of the magnitude squared of scattered amplitude shown in equation (2.51). According to equation (1.5), the scattering coefficient can be derived after further simplifications. The zero order corresponds to a planar surface, which only has specular reflection. And first order gives the incoherent field with only single scattering. Thus as stated in Kirchhoff approximation, cross-polarization scattering coefficient for backscattering is 0 due to the ignorance of multiple scattering. The first order bi-static scattering coefficient at the incident medium can be expressed as

$$\sigma_{qp} = 8|k^2 \sigma \cos\theta \cos\theta_s \alpha_{qp}|^2 W(k_x^s + k \sin(\theta_i), k_y^s) \quad (2.52)$$

where σ is the standard deviation of the surface height function, α_{qp} is defined in [23] and $W(U, V)$ is defined as

$$W(U, V) = \frac{1}{2\pi} \iint_{-\infty}^{\infty} d\xi d\zeta \exp(-jU\xi - jV\zeta) \rho(\xi, \zeta) \quad (2.53)$$

where $\rho(\xi, \zeta)$ is the correlation function of the surface. And k_x^s, k_y^s can be expressed in spherical coordinates.

$$\begin{aligned} k_x^s &= -k \sin\theta_s \cos\phi_s \\ k_y^s &= -k \sin\theta_s \sin\phi_s \end{aligned} \quad (2.54)$$

Again, backscattering from non-magnetic material is of special interest in practical applications. Mathematically, this means that $\theta_s = \theta$, $\phi_s = \pi$ and $\mu_r = 1$, leading to

$$\sigma_{qp} = 8k^4\sigma^2\cos^4\theta|\alpha_{qp}|^2W(2k\sin\theta, 0) \quad (2.55)$$

where

$$\begin{aligned} \alpha_{hh} &= R_h \\ \alpha_{vv} &= (\epsilon_r - 1) \frac{\sin^2\theta - \epsilon_r(1 + \sin^2\theta)}{[\epsilon_r\cos\theta + (\epsilon_r - \sin^2\theta)^{1/2}]^2} \\ \alpha_{hv} &= \alpha_{vh} = 0 \end{aligned} \quad (2.56)$$

As expected, cross-polarization vanishes in backscattering direction. Fortunately, if second order term is kept for both small perturbation series and Taylor expansion of exponential, we are able to obtain a non-zero cross-polarized scattering coefficient.

[24]

$$\begin{aligned} \sigma_{vh} = \sigma_{hv} &= \left[\pi k^4 \sigma^4 \cos^2\theta \frac{|(\epsilon_r - 1)(R_v - R_h)|^2}{2} \right] \\ &\quad \iint_{-\infty}^{\infty} \frac{u^2 v^2}{|D_0|^2} W(u - k\sin\theta, v) W(u + k\sin\theta, v) dudv \end{aligned} \quad (2.57)$$

where

$$D_0 = (k^2 - u^2 - v^2)^{1/2} + \epsilon_r(k^2 - u^2 - v^2)^{1/2} \quad (2.58)$$

The small perturbation method works only for slightly rough surface, and it excludes multiple scattering if this formulation is carried out in the first order. However, it has been argued that small perturbation method does account for multiple scattering up the order of expansion.[22] For example, if multiple scattering is excluded, the cross-polarization scattering coefficient is supposed to vanish in backscattering direction as shown in Kirchhoff approximation and first order small perturbation method. When second order expansion is utilized in the derivation, equation (2.57) shows that cross-polarized scattering coefficient is non-zero, which means that multiple scattering is taken into consideration in second order small perturbation method.

Table 2.1: Summary on Validity Conditions

Kirchhoff Approximation	
$kl > 6, l^2 > 2.76\sigma\lambda$	
Stationary-phase approximation	scalar approximation
$k\sigma > 2$	$k\sigma < 1, \text{rms slope} < 0.25$
Small Perturbation Method	
$k\sigma < 0.3, \text{rms slope} < 0.3$	

Another issues of small perturbation method is that energy is not conserved in first order. [20]

2.3 Range of Validity for Kirchhoff Approximation and Small Perturbation Method

In this section, validity of these two classic models will be discussed, and mathematical expression of validity under stationary isotropic Gaussian random surface is expressed.

Kirchhoff Approximation is based upon the assumption that planar reflection occurs at the every point of the surface. Thus, it requires large horizontal scale compared to wavelength and simultaneously small vertical scale roughness. This means large correlation length l and small standard deviation of surface height σ compared to wavelength is expected to fulfill the assumption. However, surface standard deviation can be comparable or even larger than the electromagnetic wavelength when the correlation length is large enough to have a small rms slope and hence a large radius of curvature is preserved. For stationary isotropic Gaussian random surfaces, the condition can be expressed mathematically as shown in Table (2.1). For stationary-phase approximation, standard deviation is required to be large, while for a scalar approximation, small standard deviation and small rms slope are desired.

While Kirchhoff model requires the horizontal-scale roughness kl to be larger than 6, surface varying horizontally with in the distance of a wavelength can be manipulated in small perturbation model. However, the surface height standard deviation is required to be much less than the electromagnetic wavelength. For stationary isotropic Gaussian stochastic processes, the validity can be shown in table (2.1). Note that if higher orders are carried out in small perturbation method, the validity range would be larger. For instance, for $k\sigma \ll 1$ and $kl > 6$, which is in the range of validity for Kirchhoff approximation, it was shown that the sum of first three orders of small perturbation method gives accurate result compared to numerical simulations. [21]

Also note that Kirchhoff approximation works for small slopes as well as small perturbation method, and thus a successful attempt to bridge this two methods is small slope approximation. [26] [25] Small slope approximation is also a widely adopted approach. [15] Nonetheless, it requires some analytical work, and cannot be implemented in computer directly. Thus, it is not discussed in this thesis.

Chapter 3

MODELING

As shown in the chapter before, two classic methods have some drawbacks. First of all, multiple scattering is not taken into consideration in Kirchhoff approximation, and in small perturbation method, multiple scattering is only taken up to the orders of expansion, which will be complicated if higher orders are carried out. Due to lack of multiple scattering, cross-polarization scattering coefficient vanishes. In addition, the range of validity of each method is limited. The proposed model can be applied to both slightly rough surfaces and rough surfaces with large correlation length.

In this chapter, integral equation is introduced at first due to the signification of this technique in both analytic and numerical methods. Then, analytic expression of surface current is obtained with the help of integral equation. And once the surface current is found, expression of far-field backscattering electric amplitude can be derived. Then, equation (1.5) is applied.

3.1 Integral Equation

Integral equation is a specific kind of equation in which the unknown variable is part of the integrand. The objective of this technique is to cast the solution for induced current density on the surface, which can be expressed in terms of integral equation. Integral equation technique, combined with numerical method such as the method of moment(MoM), finite difference time domain(FDTD) and finite element method(FEM) forms a powerful tool to solve scattering problems[28]. [1][18]

There are many classifications of integral equations and among the most widely used forms are electric field integral equation(EFIE) and magnetic field integral equa-

tion(MFIE). The EFIE enforces boundary condition on the tangential component of electric field while the boundary condition of tangential magnetic field is applied in the MFIE.

3.1.1 Electric Field Integral Equation

The boundary condition of EFIE is that total tangential field vanishes on a perfectly electric conducting(PEC) surface. And this can be expressed as

$$\begin{aligned}\vec{E}_{tan} &= \vec{E}_{tan}^i + \vec{E}_{tan}^s = 0 \quad \text{on } S \\ \vec{E}_{tan}^i &= -\vec{E}_{tan}^s \quad \text{on } S\end{aligned}\tag{3.1}$$

where S is the PEC surface, and subscript tan indicates tangential components.

With the help of scalar potential and vector potential, the scattered field can be expressed in terms of potentials which are functions of surface current density. In fact, the incident field induces surface current with current density \vec{J}_s which in turn radiates to the medium and produces the scattered field.

$$\vec{E}^s(\vec{r}) = -\nabla\Phi - j\omega\vec{A}\tag{3.2}$$

where Φ is the scalar potential and \vec{A} is the magnetic vector potential expressed as follows.

$$\vec{A}(\vec{r}) = \frac{\mu}{4\pi} \iint_S \vec{J}_s(\vec{r}') \frac{e^{-jk|\vec{r}-\vec{r}'|}}{|\vec{r}-\vec{r}'|} ds' = \mu \iint_S \vec{J}_s(\vec{r}') G(\vec{r}, \vec{r}') ds'\tag{3.3}$$

where $G(\vec{r}, \vec{r}')$ is the 3-D scalar Green's function as expressed in equation (2.9).

Lorentz gauge condition is applied in order to determine the scalar potential Φ uniquely. [4]

$$\Phi = \frac{-1}{j\omega\mu\epsilon} \nabla \cdot \vec{A}\tag{3.4}$$

Combine the above equations together, trivial calculation yields

$$\vec{E}^s(\vec{r}) = -j\frac{\eta}{k} [k^2 \iint_S \vec{J}_s(\vec{r}') G(\vec{r}, \vec{r}') ds' + \nabla \iint_S \nabla' \cdot \vec{J}_s(\vec{r}') G(\vec{r}, \vec{r}') ds']\tag{3.5}$$

where ∇ and ∇' are operator working on observation coordinates and source coordinates, respectively. And apply the boundary condition at the conducting surface,

$$\vec{E}^i(\vec{r} = \vec{r}_s) = j\frac{\eta}{k} [k^2 \iint_S \vec{J}_s(\vec{r}') G(\vec{r}_s, \vec{r}') ds' + \nabla \iint_S \nabla' \cdot \vec{J}_s(\vec{r}') G(\vec{r}_s, \vec{r}') ds'] \quad (3.6)$$

The right hand side of equation (3.6) is known incident electric field, and the unknown current density is on the left hand side and inside the integrand. Thus, this integral is referred to as electric field integral equation, and it can be used to determine the current density at any point on the surface. Once the current density is obtained, Stratton-Chu integral of current density can be employed to find the scattered field amplitude and hence the scattering coefficient.

EFIE can be applied to both open and closed surface. Note that as $|\vec{r} - \vec{r}'|$ approaches 0, there is a singularity in Green's function, which is removable in most cases. However, in EFIE, twice derivative of Green's function is taken, which gives rise to more severe singularity terms with the order of R^{-3} , and hence the integrand is not uniformly convergent.

3.1.2 Magnetic Field Integral Equation

The magnetic field integral equation is obtained through the boundary condition of tangential magnetic field.

$$\vec{J}(\vec{r}') = \hat{n} \times [\vec{H}_{tan}(\vec{r}')] = \hat{n} \times [\vec{H}^i(\vec{r}') + \vec{H}^s(\vec{r}')] \quad (3.7)$$

The scattered magnetic field can be expressed in terms of magnetic vector potential and hence as a function of induced current density.

$$\begin{aligned} \vec{H}^s(\vec{r}) &= \frac{1}{\mu} \nabla \times \vec{A} \\ &= \nabla \times \iint_S \vec{J}_s(\vec{r}') \frac{e^{-jk|\vec{r}-\vec{r}'|}}{4\pi|\vec{r}-\vec{r}'|} ds' \\ &= \nabla \times \iint_S \vec{J}_s(\vec{r}') G(\vec{r}, \vec{r}') ds' \end{aligned} \quad (3.8)$$

In the right hand of equation (3.8), differentiation can integration can be interchanged. And vector identity is utilized to simplify the expression of \vec{H}^s , which leads to

$$\nabla \times (\vec{J}_s G) = G \nabla \times \vec{J}_s - \vec{J}_s \times \nabla G \quad (3.9)$$

And two properties are applied

$$\begin{aligned} \nabla \times \vec{J}_s(\vec{r}') &= 0 \\ \nabla G &= -\nabla' G \end{aligned} \quad (3.10)$$

The above equations yield the simplified expression of scattered magnetic field.

$$\vec{H}^s(\vec{r}) = \iint_S \vec{J}_s(\vec{r}') \times \nabla G(\vec{r}, \vec{r}') ds' \quad (3.11)$$

In order to cast a solution for current density, equation (3.11) should be carried out on the conducting surface S . However, there is a singularity term inside the integrand, which can not be calculated directly. The MFIE can be expressed as a limit of this integral as \vec{r} approaches the conducting surface.

$$\vec{J}^s(\vec{r}) = \hat{n} \times H^i(\vec{r} = \vec{r}') + \lim_{\vec{r} \rightarrow S} [\hat{n} \times \iint_S \vec{J}_s(\vec{r}') \times \nabla G(\vec{r}, \vec{r}') ds'] \quad (3.12)$$

However, this equation is not applicable in most applications, since it can not be solved using numerical methods with the help of computer. Hence, an explicit form of MFIE is desired.

As shown in Figure (3.1), one can rewrite equation (3.12) as follows.

$$\vec{J}^s(\vec{r}) = \hat{n} \times H^i(\vec{r}) + \lim_{\vec{r}' \rightarrow \vec{r}} [\hat{n} \times \iint_S \vec{J}_s(\vec{r}') \times \nabla'' G(\vec{r}', \vec{r}') ds'] \quad (3.13)$$

The integral in the limit can be regarded as sum of integral over the disk D and integral over surface S other than D .

Integral over D can be expressed as

$$I_d = \lim_{\vec{r}' \rightarrow \vec{r}} [\iint_D \hat{n} \times \vec{J}_s(\vec{r}') \times \nabla'' G(\vec{r}', \vec{r}') ds'] \quad (3.14)$$

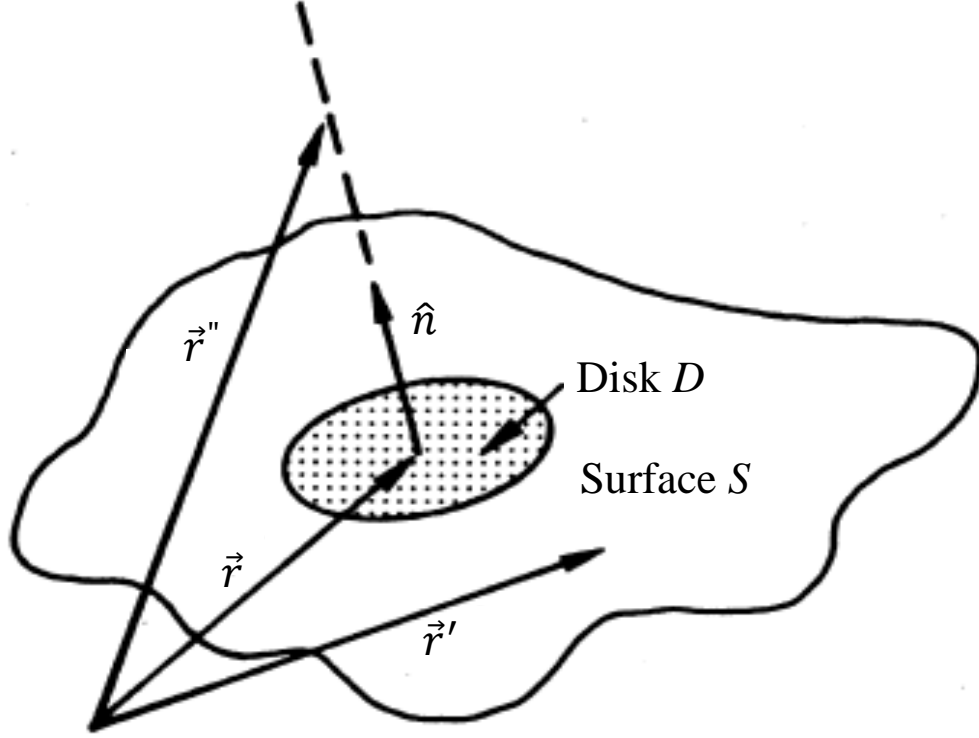


Figure 3.1: Evaluation of Limiting Value of the Integral When \vec{r}'' Approaches the Boundary

$$I_{S/D} = \iint_{S/D} \hat{n} \times \vec{J}_s(\vec{r}') \times \nabla'' G(\vec{r}'', \vec{r}') ds' \quad (3.15)$$

When D is small enough, $\vec{r}' \rightarrow \vec{r}$. And if D is small enough, equation (3.15) can be expressed as principle value integral. The following vector identity is applied

$$\hat{n} \times \vec{J}_s \times \nabla'' G = \vec{J}_s(\nabla'' G \cdot \hat{n}) - \nabla'' G(\hat{n} \cdot \vec{J}_s) \quad (3.16)$$

Since \vec{J}_s is on the surface, and \hat{n} is the normal vector of the surface, the second term on right hand side of equation (3.16) vanishes. And hence the integral over D becomes

$$I_d = \vec{J}_s(\vec{r}) \iint_D \hat{n} \cdot \nabla'' G ds' = \vec{J}_s(\vec{r}) \frac{1}{4\pi} \iint_D \frac{\hat{n} \cdot \hat{R}''}{R''^2} ds' = \vec{J}_s(\vec{r}) \frac{\Omega_D(\vec{r}'')}{4\pi} \quad (3.17)$$

where $\vec{R}'' = \vec{r}'' - \vec{r}$, R'' stands for its magnitude, and \hat{R}'' means the normalized vector \vec{R}'' . Ω_D represents the solid angle subtended by disk D at \vec{r}'' , whose value is 2π since

this disk covers half of the space.

$$\lim_{\vec{r}' \rightarrow \vec{r}} \lim_{D \rightarrow 0} I_D = \frac{\vec{J}_s(\vec{r})}{2} \quad (3.18)$$

Thus, equation (3.12) can be rearranged and rewritten as

$$\vec{J}_s(\vec{r}) = 2\hat{n} \times \vec{H}^i + \frac{1}{2\pi} \iint_{A_0} \hat{n} \times [\nabla G \times \vec{J}_s(\vec{r}')] dS' \quad (3.19)$$

Equation (3.19) is referred to as standard magnetic field integral equation, since right hand side of this integral is in terms of incident magnetic field. Note that the second integral is in terms of principle value since the disk D is not in the domain of integration.

As shown in equation (3.19), compared with equation (3.6), the MFIE has a singularity of order r^{-2} , which is better than the EFIE.[29] And this kind of singularity can be dealt with in scattering problems. [3]

3.2 Surface Current

The key to the solution of scattering from a PEC surface is the determination of surface current density. Magnetic field integral equation is utilized as our starting point to evaluate surface current density. The reason why we choose MFIE rather than EFIE is that MFIE is well-posed and converges fast. Several methods and numerical manipulations were proposed recently and convergence and fast computation time are achieved. [17] Stratton-Chu integral can be expressed as a function of surface current as shown in equation (3.20).

$$\begin{aligned} \vec{E}^s &= -C\eta\hat{k}_s \times \int_{A_0} \hat{k}_s \times \vec{J}_s e^{-j\vec{k}_s \cdot \vec{r}} dS \\ &= -C\eta\hat{k}_s \times \int_{A_0} \hat{k}_s \times \frac{\vec{J}_s}{\cos(\chi)} e^{-j\vec{k}_s \cdot \vec{r}} dx dy \end{aligned} \quad (3.20)$$

In the equation above, \vec{k}_s is the direction of scattering, η is the intrinsic impedance of free space, \hat{k}_s is the unit vector of \vec{k}_s , and C is a parameter representing circular

attenuation defined by (2.11).

Note $z = h(x, y)$ as the function of surface. Z_x and Z_y denotes the partial derivative with respect to x and y , respectively. The relations between some factors is shown in (3.21).

$$\begin{aligned}
\hat{n} &= \vec{n} \cos(\chi) \\
\vec{n} &= -\hat{x}Z_x - \hat{y}Z_y + \hat{z} \\
\cos(\chi) &= \frac{1}{\sqrt{1 + Z_x^2 + Z_y^2}} \\
dS &= \frac{dxdy}{\cos(\chi)}
\end{aligned} \tag{3.21}$$

where θ is the angle of incidence as is shown in (3.2), E_0 represents the amplitude of incident electric field. And χ is the angel between $h(x, y)$ and $x - y$ plane.

As shown in (3.20), $\vec{J}_s/\cos(\chi)$ is of interest.

$$\frac{\vec{J}_s(\vec{r})}{\cos(\chi)} = 2\vec{n} \times \vec{H}^i + \frac{1}{2\pi} \int \vec{n} \times [\nabla G \times \frac{\vec{J}_s(\vec{r}')}{\cos(\chi')}] dx' dy' \tag{3.22}$$

In the above equation, the first term at right-hand side is Kirchhoff approximation of surface current, which is used as the first guess in the integral of the second term. Since higher orders can be neglected, it is reasonable to use only first order term inside the integral.

$$\begin{aligned}
\vec{J}_{kh}(\vec{r}) &= 2\vec{n} \times \vec{H}^i \\
\vec{J}_{ch}(\vec{r}) &= \frac{1}{2\pi} \int \vec{n} \times [\nabla G \times \frac{\vec{J}_{kh}(\vec{r}')}{\cos(\chi')}] dx' dy' \\
\frac{\vec{J}_s(\vec{r})}{\cos(\chi)} &= \vec{J}_{kh}(\vec{r}) + \vec{J}_{ch}(\vec{r})
\end{aligned} \tag{3.23}$$

where J_{kh} represents Kirchhoff component, J_{ch} stands for non-Kirchhoff Component. A monochromatic, horizontal polarized incident wave can be represented as (3.24), which is taken as an example to formulate the scattering coefficient of cross-polarization,

σ_{VH} .

$$\begin{aligned}\vec{E}^i &= \hat{y} e^{k\vec{k}\cdot\vec{r}} = \hat{y} e^{-jk_x x - jk_z z} \\ &= \hat{y} e^{-jk_x \sin\theta + jk_z \cos\theta}\end{aligned}\quad (3.24)$$

where θ is the angle of incidence (Figure 3.2). In this case, \hat{y} points toward the paper, and $\hat{p} = \hat{y}$, which means this wave is horizontally polarized, or perpendicular polarized.

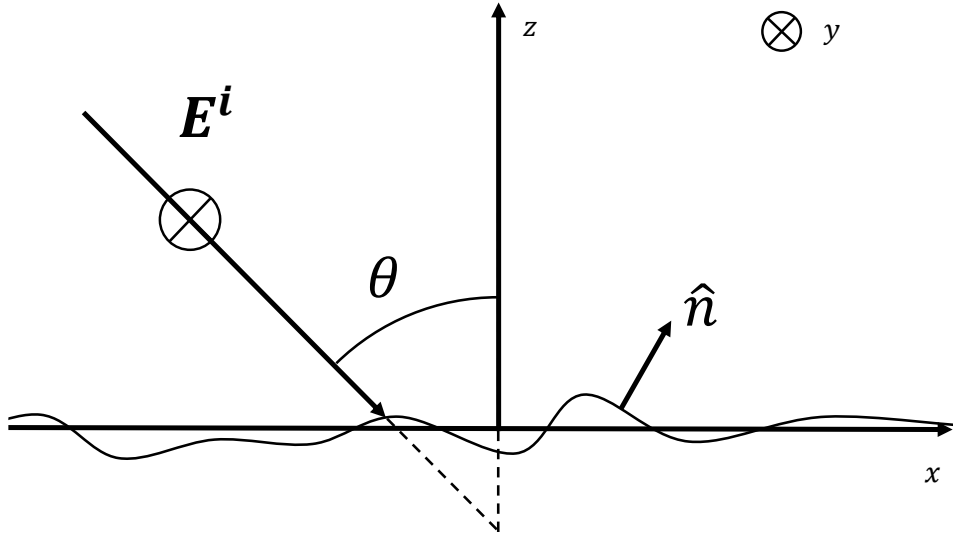


Figure 3.2: Geometry of the Surface Scattering Problem

Then, it is trivial to find J_{kh} as in (3.25)

$$J_{kh} = \frac{2E_0}{\eta} \begin{bmatrix} -Z_y \sin\theta \\ Z_x \sin\theta + \cos\theta \\ Z_y \cos\theta \end{bmatrix} e^{-jk_x x - jk_z z} \quad (3.25)$$

where Z_x, Z_y are the partial derivatives with respect to x and y , respectively.

Green's function can be expressed employing inverse Fourier transform.[3] Assume Green's function has Fourier transform \tilde{G} , and take Fourier transform of both sides

in (2.5), where $\vec{k}_0 = (u, v, q)$

$$\begin{aligned}\tilde{G}(u, v, q) &= \iiint_{-\infty}^{\infty} G(\vec{r}) e^{-j\vec{k}_0\vec{r}} dx dy dz \\ G(\vec{r}) &= \frac{1}{(2\pi)^3} \iiint_{-\infty}^{\infty} \tilde{G}(u, v, q) e^{j\vec{k}_0\vec{r}} du dv dq\end{aligned}\tag{3.26}$$

And after taking Fourier transform of two sides, and since two sides are equal for all u, v and q , we must have (3.27)

$$\begin{aligned}\tilde{G}(u, v, q) &= -\frac{1}{k_0^2 - u^2 - v^2 - q^2} \\ G(\vec{r}) &= -\frac{1}{(2\pi)^3} \iiint_{-\infty}^{\infty} \frac{1}{k_0^2 - u^2 - v^2 - q^2} e^{j\vec{k}_0\vec{r}} du dv dq\end{aligned}\tag{3.27}$$

Where $u^2 + v^2 + q^2 = k_0^2$.

Residue theorem can be applied to solve this equation, however, there are two poles in this integral, which makes this integral ambiguous since the two poles are infinity and hence not defined. This integral would be divergent without this small positive part. In practice, for every medium, there should be loss factor. Air can be modeled as a medium with very low loss in microwave frequency range, therefore, it is reasonable to assume that k_0 contains a small positive imaginary part. Namely, $k_0 = k'_0 + jk''_0$. And this introduction of k''_0 fulfills the radiation condition named limiting absorption principle.[26]

As depicted in Figure 3.3, real axis represents inverse Fourier contour, which equals to the integration along the contour C plus the residue of the pole above real axis. The two poles are off the real axis, which makes this integral unambiguously defined.

When $x > 0$, jux approaches to $-\infty$ when imaginary part of u tends to $+\infty$.

As a result, the integration along contour C vanishes according to Jordan's lemma. The whole integral(3.27) equals to the residue on the pole $\sqrt{k_0^2 - v^2 - q^2}$. Similarly, when $x < 0$, the integral(3.27) remains the same as the integrating over the pole $-\sqrt{k_0^2 - v^2 - q^2}$. All the argument yields the following equation(3.28)

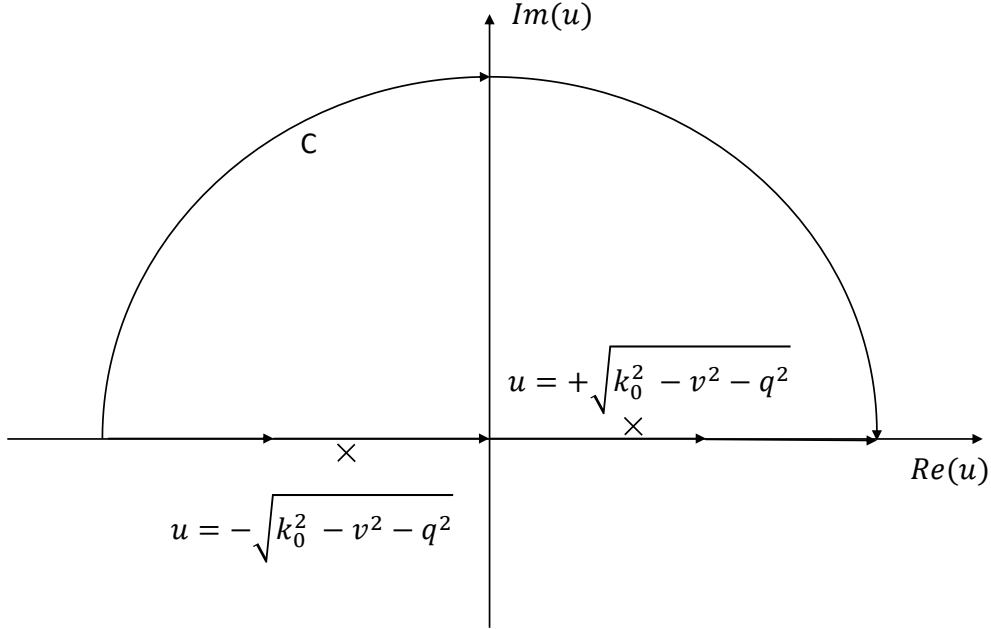


Figure 3.3: Integral Contour for Inverse Fourier Transform

$$G(\vec{r}, \vec{r}') = -\frac{j}{8\pi^2} \iint \frac{1}{u} e^{-ju|x-x'|+jv(y-y')+jq(z-z')} dv dq \quad (3.28)$$

Equation (3.28) is the same as equation (2.9), namely

$$-\frac{e^{-jk|\vec{r}-\vec{r}'|}}{4\pi|\vec{r}-\vec{r}'|} = -\frac{j}{8\pi^2} \iint \frac{1}{u} e^{-ju|x-x'|+jv(y-y')+jq(z-z')} dv dq \quad (3.29)$$

The above equation is called Weyl's identity. The physical meaning behind this identity is that a spherical wave can be reconstructed by a summation of planar wave in frequency domain. [3]

The advantage of this technique, compared to conventional Fourier transform in $x - y$ plane, is to avoid calculation of absolute value of $|z - z'|$, which is complicated. [9] In addition, z component, which is incorporated into the statistical calculation, is kept in this proposed approach. In following sections, it can be shown that the absolute value $|x - x'|$ equal to each other in symmetric case.

Hence, J_{ch} can be derived using all the equations above,

$$J_{ch} = \frac{E_0}{2\pi^2\eta} \iint dx' dy' e^{-jk_x x - jk_z z} \iint dv dq \frac{1}{u} e^{-ju|x-x'| + jv(y-y') + jq(z-z')}$$

$$\left[\begin{array}{l} \pm u Z_y \cos\theta + q Z_{y'} \sin\theta \mp u Z_{y'} \cos\theta \pm u Z_{x'} Z_y \sin\theta - v Z_y Z_{y'} \sin\theta \\ \mp u Z_x \cos\theta + v Z_{y'} \cos\theta - q Z_{x'} \sin\theta - q \cos\theta \mp u Z_x Z_{x'} \sin\theta + v Z_x Z_{y'} \sin\theta \\ -q Z_y \cos\theta \mp u Z_x Z_{y'} \cos\theta + q Z_x Z_{y'} \sin\theta - q Z_y Z_{x'} \sin\theta + v Z_y Z_{x'} \cos\theta \end{array} \right] \quad (3.30)$$

Neglecting all higher-order terms yields the following equation(3.31)

$$J_{ch} = \frac{E_0}{2\pi^2\eta} \iint dx' dy' e^{-jk_x x - jk_z z} \iint dv dq \frac{1}{u} e^{-ju|x-x'| + jv(y-y') + jq(z-z')}$$

$$\left[\begin{array}{l} \pm u Z_y \cos\theta + q Z_{y'} \sin\theta \mp u Z_{y'} \cos\theta \\ \mp u Z_x \cos\theta + v Z_{y'} \cos\theta - q Z_{x'} \sin\theta - q \cos\theta \\ -q Z_y \cos\theta \end{array} \right] \quad (3.31)$$

3.3 Far Field Backscattering Modeling

In this thesis, only cross polarization is taken into consideration since there exists many papers which provide approaches to solving RCS of like polarization. [7]

Vector identity yields an expression of \vec{E} . In this thesis, we start the computation based on the assumption that $x - x' < 0$, and as it goes with the derivation, there is no difference between $x - x' < 0$ and $x - x' > 0$ as long as the surface correlations are stationary stochastic processing. E_V lies in $x - z$ plane and only relates with x component and z component of the reflected E field.

In backscattering, the direction of scattering \vec{k}_s goes along the opposite direction of incident wave. As a result,

$$\vec{k}_s = -\hat{x}k \sin\theta + \hat{z}k \cos\theta = -\vec{k} \quad (3.32)$$

Therefore, employing vector identities, Stratton-Chu integral (3.20) can be written as

$$\vec{E}^s = -C\eta \int_{A_0} \hat{k}_s (\hat{k}_s \cdot \frac{\vec{J}_s}{\cos(\chi)}) - \frac{\vec{J}_s}{\cos(\chi)} e^{-j\vec{k}_s \cdot \vec{r}} dx dy \quad (3.33)$$

Figure 3.4 indicates E_{VH} can be computed by $\sec\theta \hat{x} \cdot \vec{E}$ or $\csc\theta \hat{z} \cdot \vec{E}$.

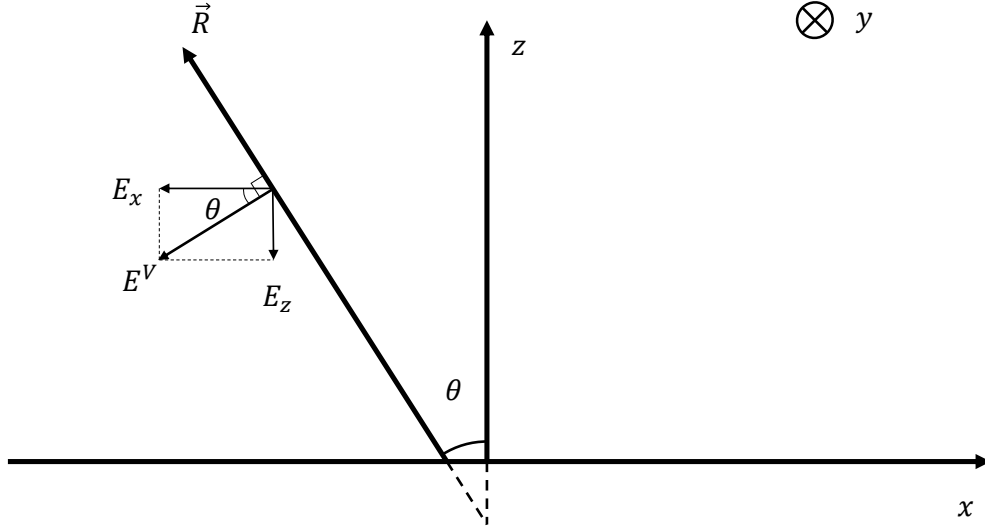


Figure 3.4: Geometry of the Reflected E Field

And these two computations give the same result. Kirchhoff component tends to vanish at E_{VH} , which is reasonable, since cross-polarization in Kirchhoff approximation is 0 for a PEC surface.

$$E_{VH} = -\frac{CE_0}{2\pi^2} \iint dvdq dx dy dx' dy' (Z_y - Z_{y'}) \cos^2\theta e^{-jk_x x - jk_z z - jk_x x' - jk_z z'} e^{ju(x-x') + jv(y-y') + jq(z-z')} \quad (3.34)$$

Integrate this integral by parts and ignore edge effects, (3.35) is obtained.

$$E_{VH} = -\frac{CE_0 \cos^2\theta}{\pi^2} \iint dvdq dx dy dx' dy' \frac{k_z v}{k_z^2 - q^2} e^{-jk_x x - jk_z z - jk_x x' - jk_z z'} e^{ju(x-x') + jv(y-y') + jq(z-z')} \quad (3.35)$$

Because q is, in most case, imaginary, it makes more sense to convert to $dudv$, and

integrate on $dudv$.

$$E_{VH} = \frac{CE_0 \cos^2 \theta}{\pi^2} \iint dudvdxdydx'dy' \frac{u}{q} \frac{k_z v}{k_z^2 - q^2} e^{-jk_x x - jk_z z - jk_x x' - jk_z z'} e^{ju(x-x') + jv(y-y') + jq(z-z')} \quad (3.36)$$

As assumed before, $q^2 = k_0^2 - u^2 - v^2$, which makes q a multi-value function, hence a careful choice of the square root branch is required. According to limiting absorption principle, k_0 has a positive imaginary part, yielding that the real part is also positive. Therefore, the square root of $k_0^2 - u^2 - v^2$ has positive real part and positive imaginary part. That is to say, q locates on the first quadrant of the complex plane, which fulfills the limiting absorption principle.

3.4 Scattered Power in Statistical Sense

Once the far-field expression is got, scattered power is needed. However, due to randomness of the surface, it is impossible to obtain an expression. The statistical average is of great interest in this case. To find the average power, we multiply E_{VH} by its complex conjugate, and then take ensemble average, namely,

$$P_{VH} = \frac{\langle E_{VH} E_{VH}^* \rangle}{\eta^2} \quad (3.37)$$

where angular brackets $\langle \rangle$ represent ensemble average over the spatial domain. And note that this P_{VH} contains circular attenuation, it is actually P_{pqr} in (1.5).

Then, after substitution, the following equation(3.38) can be deduced,

$$P = \frac{k_z^2 |C|^2 E_0^2 \cos^4 \theta}{\pi^4} \iint dx dy d\bar{x} d\bar{y} dudvd\bar{u} d\bar{v} dx' dy' d\bar{x}' d\bar{y}' \frac{u\bar{u}v\bar{v}}{q\bar{q}(k_z^2 - q^2)(k_z^2 - \bar{q}^2)} e^{jk_x(\bar{x} + \bar{x}' - x - x')} e^{ju(x-x') - j\bar{u}(\bar{x} - \bar{x}')} e^{jv(y-y') - j\bar{v}(\bar{y} - \bar{y}')} \langle e^{jk_z(\bar{z} + \bar{z}' - z - z')} e^{jq(z-z') - j\bar{q}(\bar{z} - \bar{z}')} \rangle \quad (3.38)$$

In this equation, z' and \bar{z}' are from the surfaces, while z and \bar{z} are from incident

waves. Rearrange this equation,

$$\begin{aligned}
& \langle e^{jk_z(\bar{z}+\bar{z}'-z-z')} e^{jq(z-z')-j\bar{q}(\bar{z}-\bar{z}')} \rangle \\
& = \langle e^{j(k_z-\bar{q})\bar{z}+j(-k_z-q)z'+j(-k_z+q)z+j(k_z+\bar{q})\bar{z}'} \rangle
\end{aligned} \tag{3.39}$$

It is reasonable to assume that surface variables and incident variables are independent, since physically the incident wave component does not affect surface component and vice versa. That is, the correlation coefficients $\rho_{12}, \rho_{14}, \rho_{23}$ are 0, where ρ represents correlation coefficient, and 1,2,3,4 stand for \bar{z}, z', z, \bar{z}' respectively. In addition, it is natural to assume that the correlation between \bar{z} and z and the correlation between \bar{z}' and z' are identical, since it is a dual relationship. The following equation(3.40) can be derived because of independence.

$$\begin{aligned}
& \langle e^{j(k_z-\bar{q})\bar{z}+j(-k_z-q)z'+j(-k_z+q)z+j(k_z+\bar{q})\bar{z}'} \rangle \\
& = \langle e^{j(k_z-\bar{q})\bar{z}+j(-k_z+q)z} \rangle \langle e^{j(-k_z-q)z'+j(k_z+\bar{q})\bar{z}'} \rangle \\
& = e^{-\sigma^2[2k_z^2+q^2+\bar{q}^2+(k_z\bar{q}-q\bar{q}-k_z^2+k_zq)\rho_{13}+(-k_zq-k_z\bar{q}-q\bar{q}-k_z^2)\rho_{24}]}
\end{aligned} \tag{3.40}$$

Substitute (3.40) to (3.38), the expression of power can be simplified.

$$\begin{aligned}
P & = \frac{k_z^2|C|^2E_0^2\cos^4\theta}{\pi^4} \iint dxdyd\bar{x}d\bar{y}dudvd\bar{u}d\bar{v}dx'dy'd\bar{x}'d\bar{y}' \frac{u\bar{u}v\bar{v}}{q\bar{q}(k_z^2-q^2)(k_z^2-\bar{q}^2)} \\
& \quad e^{jk_x(\bar{x}+\bar{x}'-x-x')} e^{ju(x-x')-j\bar{u}(\bar{x}-\bar{x}')} e^{jv(y-y')-j\bar{v}(\bar{y}-\bar{y}')} \\
& \quad e^{-\sigma^2[2k_z^2+q^2+\bar{q}^2+(k_z\bar{q}-q\bar{q}-k_z^2+k_zq)\rho_{13}+(-k_zq-k_z\bar{q}-q\bar{q}-k_z^2)\rho_{24}]}
\end{aligned} \tag{3.41}$$

It would be convenient to change into a different coordinates, $x - \bar{x} = \xi$, $y - \bar{y} = \eta$, $x' - \bar{x}' = \zeta$, $y' - \bar{y}' = \tau$. These are the distances, and for stationary stochastic process, the correlation coefficient is only a function of the distance. Therefore, this substitution would simplify the calculation.

$$\begin{aligned}
P & = \frac{k_z^2|C|^2E_0^2\cos^4\theta}{\pi^4} \iint d\xi d\eta d\zeta d\tau d\bar{x}d\bar{y}d\bar{x}'d\bar{y}' dudvd\bar{u}d\bar{v} \frac{u\bar{u}v\bar{v}}{q\bar{q}(k_z^2-q^2)(k_z^2-\bar{q}^2)} \\
& \quad e^{-jk_x(\xi+\zeta)-ju(\zeta-\xi)-jv(\tau-\eta)} e^{j(u-\bar{u})(\bar{x}-\bar{x}')+j(v-\bar{v})(\bar{y}-\bar{y}')} \\
& \quad e^{-\sigma^2[2k_z^2+q^2+\bar{q}^2+(k_z\bar{q}-q\bar{q}-k_z^2+k_zq)\rho_{13}+(-k_zq-k_z\bar{q}-q\bar{q}-k_z^2)\rho_{24}]}
\end{aligned} \tag{3.42}$$

Dirac-delta function can be applied in order to simplify this equation.(3.43)

$$\int e^{j(u-\bar{u})\bar{x}} d\bar{x} = 2\pi\delta(u - \bar{u}), \quad \int e^{j(v-\bar{v})\bar{y}} d\bar{y} = 2\pi\delta(v - \bar{v}) \quad (3.43)$$

Only when $\bar{u} = u$ and $\bar{v} = v$, this integral is nonzero. Therefore, \bar{u} and \bar{v} can be eliminated by the introduction of Dirac-delta function.

$$\iint e^{j(u-\bar{u})(\bar{x}-\bar{x}')} e^{j(v-\bar{v})(\bar{y}-\bar{y}')} d\bar{x}d\bar{y}d\bar{x}'d\bar{y}' = 4\pi^2 \iint d\bar{x}'d\bar{y}' = 4\pi^2 A_0 \quad (3.44)$$

In addition, Dirac-delta function gives us that $u = \bar{u}$ and $v = \bar{v}$, which implies that $q^2 = \bar{q}^2$. In fact, \bar{q} equals to complex conjugate of q . Hence, the entire integral can be expressed as (3.45)

$$P = \frac{4k_z^2|C|^2 A_0 E_0^2 \cos^4\theta}{\pi^2} \iint d\xi d\eta d\zeta d\tau dudv \frac{u^2 v^2}{q\bar{q}(k_z^2 - q^2)^2} e^{-jk_x(\xi+\zeta)-ju(\zeta-\xi)-jv(\tau-\eta)} e^{-\sigma^2[2k_z^2+2q^2-(k_z-\bar{q})(k_z-q)\rho_{13}-(k_z+q)(k_z+\bar{q})\rho_{24}]} \quad (3.45)$$

Note that $q^2 = \bar{q}^2$ does not necessarily imply $q = \bar{q}$. ρ_{13} is a function of ζ and ξ , while ρ_{24} is a function of η and τ .

In order to obtain incoherent power, we subtract the mean-square value from the power, yielding

$$P - P_{ms} = \langle E_{VH} E_{VH}^* \rangle - \langle E_{VH} \rangle^2 = \frac{4k_z^2|C|^2 A_0 E_0^2 \cos^6\theta}{\pi^2} \iint d\xi d\eta d\zeta d\tau dudv \frac{u^2 v^2}{q\bar{q}(k_z^2 - q^2)^2} e^{-jk_x(\xi+\zeta)-ju(\zeta-\xi)-jv(\tau-\eta)} e^{-\sigma^2(2k_z^2+2q^2)} (e^{\sigma^2[(k_z-\bar{q})(k_z-q)\rho_{13}+(k_z+q)(k_z+\bar{q})\rho_{24}]} - 1) \quad (3.46)$$

Expand exponential term by Taylor series,

$$e^{\sigma^2[(k_z-\bar{q})(k_z-q)\rho_{13}+2(k_z+q)(k_z+\bar{q})\rho_{24}]} = \sum_{m=0}^{\infty} \sum_{n=0}^{\infty} \frac{\sigma^{2(m+n)} (k_z - \bar{q})^m (k_z - q)^m (k_z + q)^n (k_z + \bar{q})^n}{m!n!} \rho_{13}^m \rho_{24}^n; \quad (3.47)$$

For $m = n = 0$, this equation is 1, canceling the mean square value. In addition, for $m = 0, n \neq 0$ or $m \neq 0, n = 0$, it can be found that the RCS is zero due to the

existence of Dirac-delta function. Namely, for $m = 0$, the expression contains $\delta(u)$ and therefore $u = 0$ is taken in the integral, which implies the whole expression is 0. Similarly, we can conclude that for $n = 0$, this integral vanishes. Thus, the first order is $m = n = 1$.

A definition of new function W will be employed throughout this thesis.

$$W^n(U, V) = \frac{1}{2\pi} \iint_{-\infty}^{\infty} d\xi d\zeta \exp(-jU\xi - jV\zeta) \rho^n(\xi, \zeta) \quad (3.48)$$

where n denotes the n th power of ρ .

Note that if $n = 1$, equation(2.53) shows that this is the Fourier transform of the surface correlation function, which is called roughness spectrum of the surface.

Scattering coefficient is expressed by (1.5). And G_t is assumed to be 1 in order to simplify the calculations. After simplifications, the following equation(3.49) can be derived.

$$\sigma_{VH}^0 = \frac{4\pi R^2}{A_0 E_0^2 \eta^2} (\langle E_{VH} E_{VH}^* \rangle - \langle E_{VH} \rangle^2) \quad (3.49)$$

Hence, the power can be expressed in term of W^n , and after trivial calculation,

$$\begin{aligned} \sigma_{VH}^0 &= \frac{4k^4 \cos^6 \theta}{\pi} \sum_{m=1}^{\infty} \sum_{n=1}^{\infty} \int_{R^2} dudv \frac{u^2 v^2}{q\bar{q}(k_z^2 - q^2)^2} e^{-\sigma^2(2k_z^2 + 2q^2)} \\ &\frac{\sigma^{2(m+n)} (k_z - \bar{q})^m (k_z - q)^m (k_z + q)^n (k_z + \bar{q})^n}{m!n!} W^m(k \sin \theta - u, -v) W^n(k \sin \theta + u, v) \end{aligned} \quad (3.50)$$

Follow the same procedure, assume $x - x > 0'$, then another equation of RCS can be computed as (3.51) In fact, the x component and z component of E_{VH} only differ by sign, which can be eliminated by taking square of E_{VH} . And throughout the derivation, it has nothing but the sign to do with the ensemble average, after similar

calculation, (3.51) can be deduced.

$$\sigma_{VH}^0 = \frac{4k^4 \cos^6 \theta}{\pi} \sum_{m=1}^{\infty} \sum_{n=1}^{\infty} \int_{R^2} dudv \frac{u^2 v^2}{q\bar{q}(k_z^2 - q^2)^2} e^{-\sigma^2(2k_z^2 + 2q^2)} \frac{\sigma^{2(m+n)}(k_z - \bar{q})^m (k_z - q)^m (k_z + q)^n (k_z + \bar{q})^n}{m!n!} W^m(k \sin \theta + u, -v) W^n(k \sin \theta - u, v) \quad (3.51)$$

Compare (3.50) and (3.51), it is obvious that if (3.52) holds, then these two expressions are identical when $m = n$.

$$W(k \sin \theta + u, -v) W(k \sin \theta - u, v) = W(k \sin \theta - u, -v) W(k \sin \theta + u, v) \quad (3.52)$$

A stationary random processing is defined in the way that the autocorrelation function only depends on the distance. Therefore, the correlation function is an even function, which implies that its Fourier transform is even(3.53).

$$\begin{aligned} W(k \sin \theta + u, -v) &= W(k \sin \theta + u, v) \\ W(k \sin \theta - u, v) &= W(k \sin \theta - u, -v) \end{aligned} \quad (3.53)$$

We can conclude that if the surface is stationary stochastic processing, then these two equations have the same result when $m = n$. The assumption here makes sense if it is used to model sea surface. Physically, sea surface is big enough to be modeled as a infinite surface. The correlation between two points on the sea surface depend only on the distance if we exclude the influence of wind. Ideally, x direction and y direction has the same distribution.

And since the first order dominates the result, to simplify the calculation, higher orders are ignored in this approach. Stationary stochastic processing is utilized in this thesis, and keeping the lowest order, the two situations have the same results. Therefore, the probability of each case is not important in this situation. In conclusion, this equation works for stationary isotropic random processes.

NUMERICAL EVALUATION, RESULTS, AND FUTURE WORK

4.1 Numerical Method to Evaluate the Integral

In this section, the evaluation of the integral (3.51) is proposed. In order to validate this method, Gaussian distribution is assumed for both x and y direction. And only first order item is kept in order to simplify the numerical evaluation. All higher orders are neglected since that W^n is of higher orders. Ignore all higher orders, the integral(3.51) can be expressed by

$$\sigma_{VH}^0 = \frac{4k^4\sigma^4\cos^6\theta}{\pi} \int_{R^2} dudv \frac{u^2v^2}{q\bar{q}} e^{-\sigma^2(2k_z^2+2q^2)} W(k\sin\theta - u, -v)W(k\sin\theta + u, v) \quad (4.1)$$

Since \bar{q} comes from E_{VH}^* , $\bar{q} = q^*$. Hence, the equation becomes (4.2)

$$\sigma_{VH}^0 = \frac{4k^4\sigma^4\cos^6\theta}{\pi} \int_{R^2} dudv \frac{u^2v^2}{|q|^2} e^{-\sigma^2(2k_z^2+2q^2)} W(k\sin\theta - u, -v)W(k\sin\theta + u, v) \quad (4.2)$$

For Gaussian isotropic random process, the correlation function can be expressed as follows

$$\rho(\xi, \zeta) = e^{-\frac{\xi^2+\zeta^2}{l^2}} \quad (4.3)$$

Hence, according to equation (3.48), W^n can be expressed as follows for Gaussian correlation

$$W^n(U, V) = \frac{1}{2\pi} \iint_{-\infty}^{\infty} d\xi d\zeta e^{-jU\xi - jV\zeta} e^{-n(\frac{\xi^2+\zeta^2}{l^2})} \quad (4.4)$$

Evaluate the above integral using change of variables, we can get

$$W^n(U, V) = \frac{l^2}{2n} \exp\left[-\frac{(U^2 + V^2)l^2}{4n}\right] \quad (4.5)$$

Substitute equation (4.5) into equation (4.2), one can get

$$\sigma_{VH}^0 = \frac{4k^4\sigma^4\cos^6\theta}{\pi} \int_{R^2} dudv \frac{u^2v^2}{|q|^2} e^{-\sigma^2(2k_z^2+2q^2)} \frac{l^4}{4} \exp\left[-\frac{l^2(k^2\sin^2\theta + u^2 + v^2)}{2}\right] \quad (4.6)$$

Normalization of u , v and q gives further simplification of the integral. And one benefit of normalization is that kl terms are carried out.

$$\sigma_{VH}^0 = \frac{k^4\sigma^4k^4l^4\cos^6\theta}{\pi} e^{-2k^2\sigma^2\cos^2\theta} e^{-\frac{k^2l^2(1+\sin^2\theta)}{2}} \int_{R^2} dudv \frac{u^2v^2}{|q|^2} e^{\frac{k^2l^2q^2}{2}} e^{-2q^2(k\sigma)^2} \quad (4.7)$$

where $u^2 + v^2 + q^2 = 1$ in equation (4.7) due to normalization.

However, equation (4.7) has a singularity due to the singularity for Green's function in lossless medium. And once we convert this equation into polar coordinates of u, v and simplify it by change of variables, as shown in equation(4.9), this singularity is a logarithmic branch-point singularity. Note that $\rho^2 = u^2 + v^2$.

$$\sigma_{VH}^0 = \frac{k^4\sigma^4k^4l^4\cos^6\theta}{4} e^{-2k^2\sigma^2(1+\cos^2\theta)} e^{-\frac{k^2l^2\sin^2\theta}{2}} \int_0^\infty d\rho \frac{\rho^5}{|1-\rho^2|} e^{-\frac{k^2l^2\rho^2}{2}} e^{+2\rho^2(k\sigma)^2} \quad (4.8)$$

Further simplification can be made by making $\varrho = \rho^2$, yielding

$$\sigma_{VH}^0 = \frac{k^4\sigma^4k^4l^4\cos^6\theta}{8} e^{-2k^2\sigma^2(1+\cos^2\theta)} e^{-\frac{k^2l^2\sin^2\theta}{2}} \int_0^\infty d\varrho \frac{\varrho^2}{|1-\varrho|} e^{-\frac{k^2l^2\varrho}{2}} e^{+2\varrho(k\sigma)^2} \quad (4.9)$$

Note that when $|q| = 1$, the term in the integrand is non-convergent and thus, it is impossible to do numerical integration. Recall that convergence and uniqueness is guaranteed by the introduction of small loss and hence the fulfillment of radiation condition. Or on the other hand, the path of integral is stipulated for the evaluation of this integral and Sommerfeld integration path is one of the most widely adopted. [3]

Sommerfeld adopted the path as shown in Figure(4.1), which is a path located on the complex plane, and this path worked even for lossless medium. However,

it only works for theoretical purpose. There are several methods dealing with the evaluation of Sommerfeld integral. And method of uniform asymptotic expansions is one of the most widely adopted approaches, despite the weakness that this method is problem specific. One way of computing the solution to these kinds of problems in a general case is by the numerical integration of Sommerfeld integration. An advantage of numerical evaluation is that it is capable to a computer program and hence applicable widely.

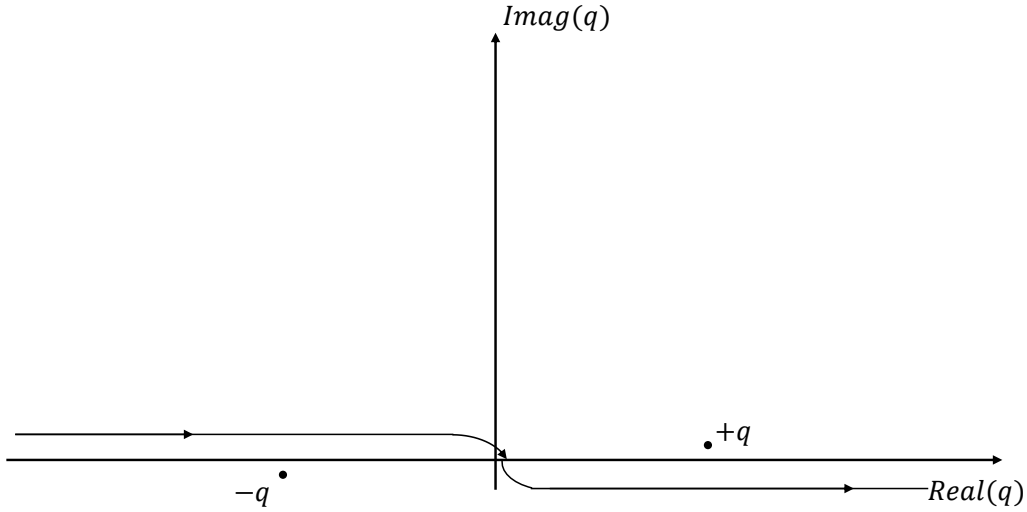


Figure 4.1: Sommerfeld Integration Path in Complex q Plane

Numerically, since there could be singularities on the real axis, the integrand in a vicinity of the singularity will be sharp peaked, which exacerbates the errors in numerical evaluation. Thus, we choose an integration path as shown in figure (4.2).

Since the singularities are assumed to have some positive imaginary part in order to ensure radiation condition, there is no singularity in the positive real axis. Thus, the proposed integration path has the same value as the original integral according to Cauchy's integral theorem as long as the value of the integrand equals 0 at infinity.

As shown in figure (4.2), numerically integrating the integral along an integration path parallel to the real axis is the way adopted in this thesis for ease of implemen-

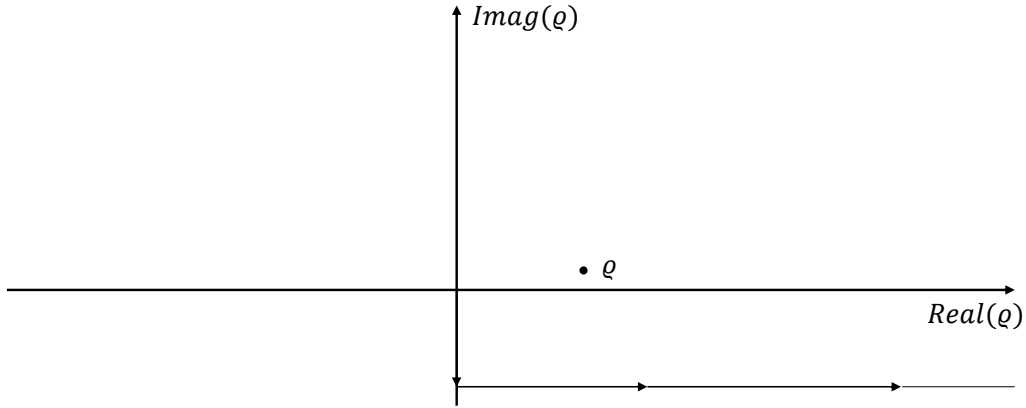


Figure 4.2: A Robust Way of Defining an Integration Path

tation on computers.

There are several choices of integral path in order to evaluate equation (4.9). And there are several advantages of this particular path. First of all, this choice of integration path avoids the sharp peak caused by singularity, making the integrand smoother and converge faster. Then, this integration path is simple for computer simulation. In addition, this integration path is a robust path since the error committed in a numerical scheme is proportional to the derivatives of the integrand. Adaptive integration techniques can interpolation techniques can be applied in this integration path to evaluate this kind of integral.[3]

And note that the integration path is valid only when the value of the integrand vanishes at infinity. A sufficient condition for this is $(kl)^2 > 4(k\sigma)^2$, which means the exponential term inside the integral decays when ϱ approaches $+\infty$. According to equation (1.1), this condition means that

$$m = \sqrt{2} \frac{\sigma}{l} < \frac{1}{\sqrt{2}} \quad (4.10)$$

Equation (4.10) shows one of the restrictions on the range of validity of this proposed model. However, for both Kirchhoff approximation and small perturbation method,

rms slope is required to be less than 0.5 typically. So this condition is of practical use.

4.2 Results and Comparison with Classic Model

After numerical integration path is established, equation (4.9) can be evaluated by the aid of computer program. And equation (2.57) is used for comparison, assuming $\epsilon_r = 1 - j20000$ for the dielectric. Since a dielectric material with large electric coefficient can be regarded as a good conductor in the sense of Fresnel reflection coefficient.

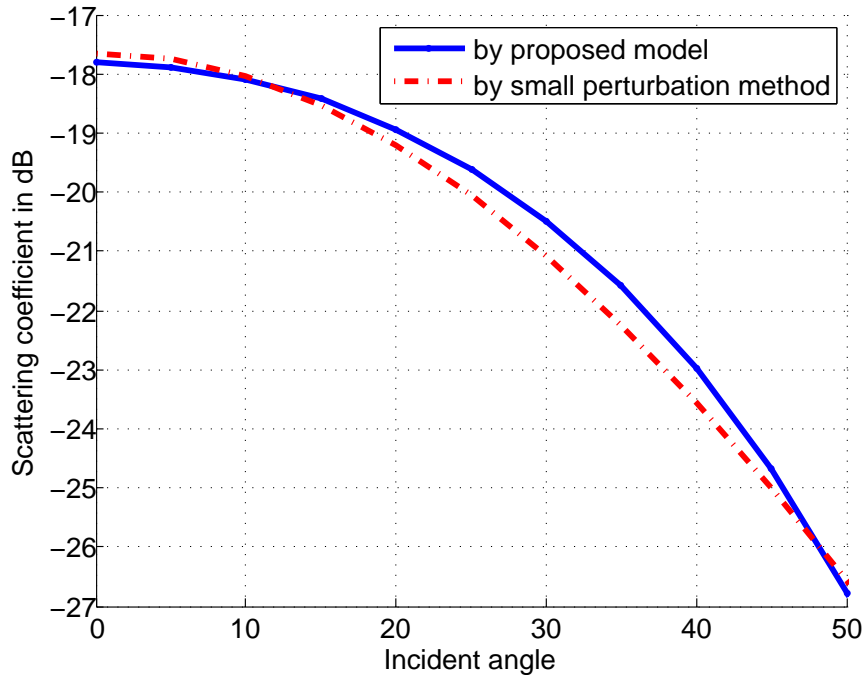


Figure 4.3: The Scattering Coefficient for $k\sigma = 0.2$ and $kl = 2.0$

As shown in Figure (4.3), the scattering coefficient decreases as incident angle increases, due to decrease of Fresnel reflection coefficient as incident angle increases. Only angles from 0 degree to 50 degrees are considered in this thesis, since large inci-

dent angle means small grazing angle. And a large amount of incident wave is shadowed and multiple scattering takes place, such that it is not accurate. Fortunately, in practice remote sensing applications, small grazing angle is not of interest since transmitter and receiver antenna are usually carried on a plane or satellite, which is high from the earth surface. And also note that as grazing angle get smaller, scattering coefficient from perturbation method is larger because of ignorance of shadowing and higher-order multiple scattering.

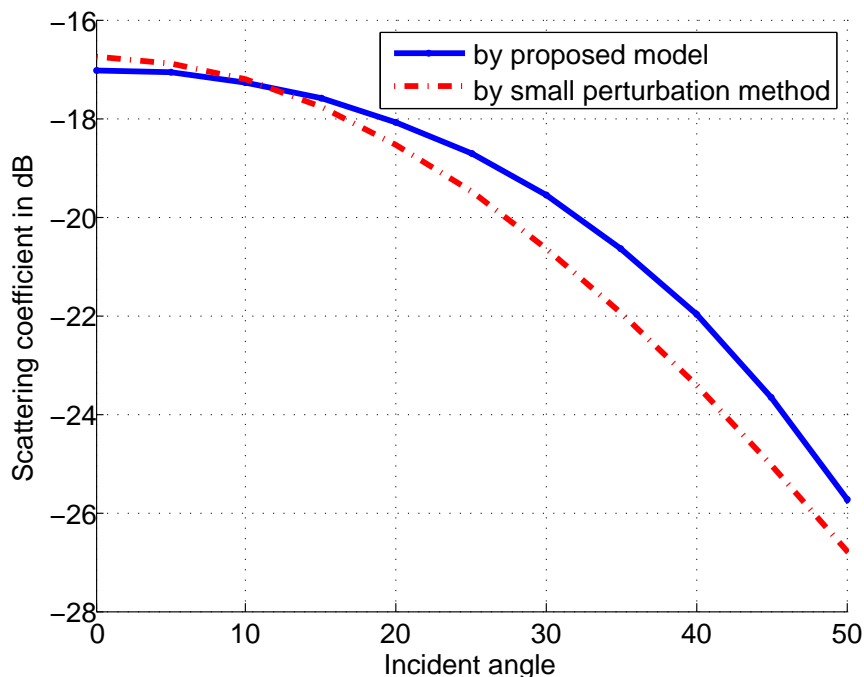


Figure 4.4: The Scattering Coefficient for $k\sigma = 0.2$ and $kl = 2.4$

As shown in Figure (4.4), the shape of this curve is similar to the curve shown in Figure (4.3). However, in this situation, scattering coefficient is larger than $kl = 2.0$. In addition, when grazing angle gets smaller, the difference between these two methods gets smaller. For fixed height variation, larger correlation length means smaller rms slope, which implies that multiple scattering and shadowing are not as severe as larger

slope surfaces. And since shadowing gets smaller, the scattering field in backscattering direction gets more power, and hence larger scattering coefficient.

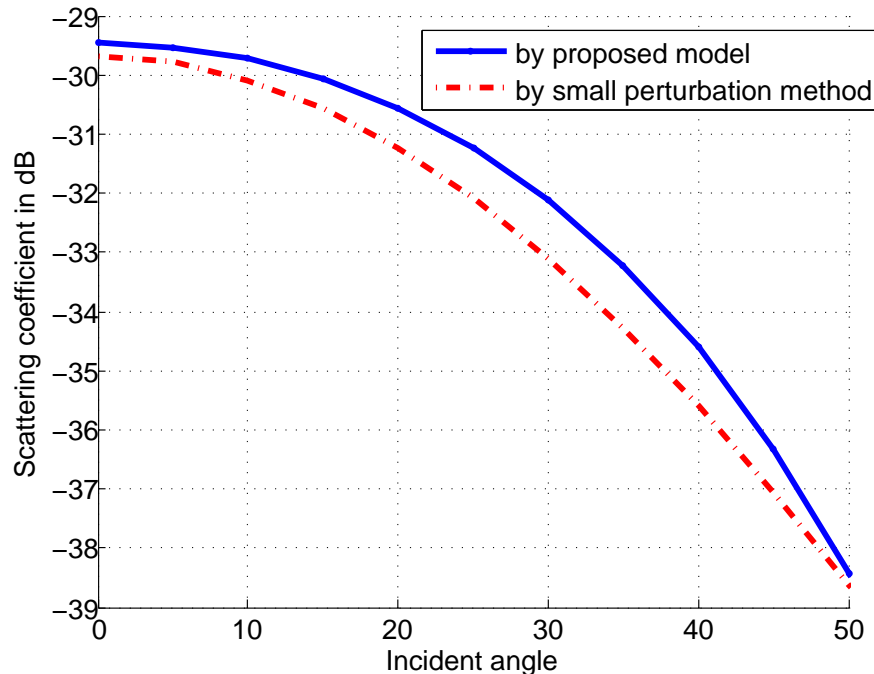


Figure 4.5: The Scattering Coefficient for $k\sigma = 0.1$ and $kl = 2.0$

As shown in Figure (4.5), as standard deviation increases, the value of backscattering coefficient gets raised near vertical direction. As the rms slope increases, second order multiple scattering begins to contribute more into the total scattering coefficient, and thus large scattering coefficient is expected.

Above figures indicate that the scattering coefficient agree well with the small perturbation method.

Note that scattering coefficient given by proposed model is larger than it given by equation (2.57). The main reason is that in equation (2.57), a dielectric with large imaginary permittivity is used to approximate a PEC surface. However, though it can form a very good conductor, it is impossible to get perfect conducting.

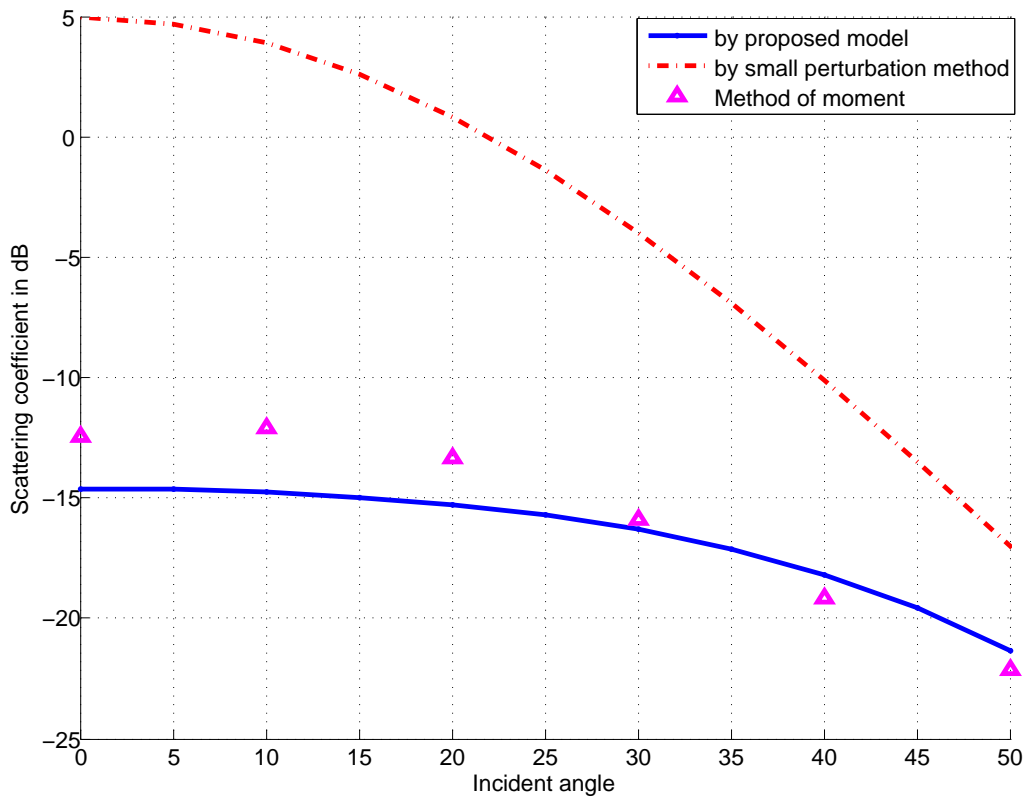


Figure 4.6: The Scattering Coefficient for $k\sigma = 1.26$ and $kl = 3.77$

Figure (4.6) depicts that the proposed model works for intermediate range, by comparison with numerical method for a dielectric with large loss tangent. [12]. This set of surface is out of the range of validity of both small perturbation method and Kirchhoff approximation, and the proposed model achieves good agreement with numerical simulation.

4.3 Conclusion and Future Work

As shown in above figures, the proposed model agrees well with small perturbation method carried out to second order in relatively large grazing angle. In addition, this proposed model has larger range of validity since it works for intermediate range. However, the validity condition of this model is required in order to be applied in

practice. The comparison with rough surface as in Kirchhoff model range is desired to show the agreement and validity of this model in high frequency range.

REFERENCES

- [1] Constantine A Balanis. *Advanced engineering electromagnetics*. John Wiley & Sons, 1999.
- [2] Constantine A. Balanis. *Antenna theory: analysis and design*. John Wiley & Sons, third edition, 2005.
- [3] Weng Cho Chew. *Waves and fields in inhomogeneous media*, volume 522. IEEE Press New York, 1995.
- [4] K Cheng David. *Field and wave electromagnetics*. 1983.
- [5] T. M. Elfouhaily and J. T. Johnson. A new model for rough surface scattering. *IEEE Transactions on Geoscience and Remote Sensing*, 45(7):2300–2308, July 2007.
- [6] Tanos Elfouhaily, Stephan Guignard, Ra’id Awadallah, and Donald R Thompson. Local and non-local curvature approximation: a new asymptotic theory for wave scattering. *Waves in Random Media*, 13(4):321–337, 2003.
- [7] A.K. Fung and G.W. Pan. A scattering model for perfectly conducting random surfaces i. model development. *International Journal of Remote Sensing*, 8(11):1579–1593, 1987.
- [8] C. A. Gurin and J. T. Johnson. A simplified formulation for rough surface cross-polarized backscattering under the second-order small-slope approximation. *IEEE Transactions on Geoscience and Remote Sensing*, 53(11):6308–6314, Nov 2015.
- [9] A Ishimaru, C Le, Y Kuga, LA Sengers, and TK Chan. Polarimetric scattering theory for high slope rough surface. *Progress In Electromagnetics Research*, 14:1–36, 1996.
- [10] J. T. Johnson and J. D. Ouellette. Polarization features in bistatic scattering from rough surfaces. *IEEE Transactions on Geoscience and Remote Sensing*, 52(3):1616–1626, March 2014.
- [11] Joel T. Johnson. Third-order small-perturbation method for scattering from dielectric rough surfaces. *J. Opt. Soc. Am. A*, 16(11):2720–2736, Nov 1999.
- [12] M. Kuzuoglu and O. Ozgun. A numerical model for investigating the effect of rough surface parameters on radar cross section statistics. In *2017 IEEE International Symposium on Antennas and Propagation USNC/URSI National Radio Science Meeting*, pages 1837–1838, July 2017.
- [13] J. Li, M. Zhang, P. Wei, and W. Jiang. An improvement on ssa method for EM scattering from electrically large rough sea surface. *IEEE Geoscience and Remote Sensing Letters*, 13(8):1144–1148, Aug 2016.

- [14] T. H. Liao, L. Tsang, S. Huang, N. Niamsuwan, S. Jaruwatanadilok, S. b. Kim, H. Ren, and K. L. Chen. Copolarized and cross-polarized backscattering from random rough soil surfaces from L-Band to Ku-Band using numerical solutions of maxwell's equations with near-field precondition. *IEEE Transactions on Geoscience and Remote Sensing*, 54(2):651–662, Feb 2016.
- [15] L. Linghu, Z. Wu, X. Guo, H. Li, and W. Bin. Small-slope approximation for electromagnetic wave scattering at the dielectric rough sea surface. In *ISAPE2012*, pages 815–818, Oct 2012.
- [16] G. G. Pan, M. Jin, L. Zhang, M. Bai, and J. Miao. An efficient scattering algorithm for smooth and sharp surfaces: Coiflet-based scalar MFIE. *IEEE Transactions on Antennas and Propagation*, 62(8):4241–4250, Aug 2014.
- [17] G. G. Pan, M. Jin, L. Zhang, M. Bai, and J. Miao. An efficient scattering algorithm for smooth and sharp surfaces: Coiflet-based scalar MFIE. *IEEE Transactions on Antennas and Propagation*, 62(8):4241–4250, Aug 2014.
- [18] George W Pan. *Wavelets in electromagnetics and device modeling*, volume 159. John Wiley & Sons, 2003.
- [19] Stephen O Rice. Reflection of electromagnetic waves from slightly rough surfaces. *Communications on pure and applied mathematics*, 4(2-3):351–378, 1951.
- [20] J. T. Johnson T. Wang, L. Tsang and S. Tan. Scattering and transmission of waves in multiple random rough surfaces: energy conservation studies with the second order small perturbation method. *Progress In Electromagnetics Research*, 157:1–20, 2016.
- [21] Eric I Thorsos and Darrell R Jackson. Studies of scattering theory using numerical methods. *Waves in Random Media*, 1(3):S165–S190, 1991.
- [22] F Ticconi, L Pulvirenti, and N Pierdicca. Models for scattering from rough surfaces. *Electromagnetic Waves*, 2011.
- [23] Fawwaz T Ulaby, Richard K Moore, and Adrian K Fung. Microwave remote sensing active and passive-volume ii: Radar remote sensing and surface scattering and emission theory. 1982.
- [24] G Valenzuela. Depolarization of EM waves by slightly rough surfaces. *IEEE Transactions on Antennas and Propagation*, 15(4):552–557, 1967.
- [25] A Voronovich. Small-slope approximation for electromagnetic wave scattering at a rough interface of two dielectric half-spaces. *Waves in Random Media*, 4(3):337–367, 1994.
- [26] Alexander G Voronovich. *Wave scattering from rough surfaces*, volume 17. Springer Science & Business Media, 2013.

- [27] F. Xu and P. Wang. Analytical modeling of rough surface SAR images under small perturbation approximation. *IEEE Transactions on Geoscience and Remote Sensing*, 55(7):3694–3707, July 2017.
- [28] L. Zhang, G. Pan, and J. Jones. A general scattering algorithm for dielectric and PEC random rough surfaces. In *2016 IEEE Conference on Antenna Measurements Applications (CAMA)*, pages 1–4, Oct 2016.
- [29] L. Zhang, G. Pan, and J. Jones. Study of fast mfi for closed-surface target scattering in antenna system. In *2016 IEEE Conference on Antenna Measurements Applications (CAMA)*, pages 1–4, Oct 2016.
- [30] L. Zhang, G. G. Pan, and J. A. Jones. On unified numerical algorithm for 3-d scattering from dielectric and PEC random rough surfaces. *IEEE Transactions on Antennas and Propagation*, 65(5):2615–2623, May 2017.